A review of paramylon processing routes from microalga biomass to non-derivatized and chemically modified products

Frédérica Feuzing, Jean Pierre Mbakidi, Luc Marchal, Sandrine Bouquillon, Eric Leroy

A review of paramylon processing routes from microalga biomass to non-derivatized and chemically modified products.

Frédérica Feuzing,[a,b] Jean Pierre Mbakidi,[b] Luc Marchal,[a] Sandrine Bouquillon,[b] Eric Leroy,[a,*]

[a] Université de Nantes, Oniris, CNRS, GEPEA, UMR 6144, F- 44470 Carquefou, France.

[b] Institut de Chimie Moléculaire de Reims, CNRS UMR 7312, Université de Reims Champagne-Ardenne, BP 1039, 51687 Reims Cedex, France

* Corresponding author: eric.leroy@univ-nantes.fr

Abstract

Paramylon is a linear β-1,3-glucan, similar to curdlan, produced as intracellular granules by the microalga *Euglena gracilis*, a highly versatile and robust strain, able to grow under various trophic conditions, with valorization of CO_2, wastewaters, or food byproducts as nutrients. This review focuses in particular on the various processing routes leading to new potential paramylon based products. Due to its crystalline structure, involving triple helices stabilized by internal intermolecular hydrogen bonds, paramylon is neither water-soluble nor thermoplastic. The few solvents able to disrupt the triple helices, and to fully solubilize the polymer as random coils, allow non derivatizing shaping into films, fibers, and even nanofibers by a specific self-assembly mechanism. Chemical modification in homogeneous or heterogeneous conditions is also possible. The non-selective or regioselective substitution of the hydroxyl groups of glucosidic units leads to water-soluble ionic derivatives and thermoplastic paramylon esters with foreseen applications ranging from health to bioplastics.

Keywords: β-1,3-glucan, crystallinity, solvents, processing, chemical modification.

Introduction

Among the natural glucans (defined in this review as polysaccharides that are homopolymers of glucose) that possess a linear macromolecular structure, those involving β-1,3 linkages between glycosidic repeating units are the scarcest. Contrary to cellulose, involving β-1,4 linkages, or amylose from starch, based on α-1,4 linkages, which are referred to by the same names whatever was their botanical, bacterial, or fungal origin; linear β-1,3-glucans have been given different names depending on their origin, the most common being curdlan and paramylon (Stone, 2009): paramylon is a storage polysaccharide deposited as microscopic granules in the cytoplasm of euglenoids, in particular the microalga *Euglena gracilis* (abbreviated *E. gracilis* in the following). It was discovered in 1850 by German Professor J. Gottlieb who named it. "paramylon" associates the two latin words « par » (standing by) and « amylon » (starch)) (Kiss et al., 1987; Barsanti et al., 2011), because besides being an isomer of starch, with a similar granule form, it is not stained by iodine (Clarke & Stone, 1960). Despite this early discovery, paramylon remained a laboratory curiosity for a long time.

In contrast, curdlan was discovered in 1966 during studies of exopolysaccharides production by bacterium *Alcaligene faecalis* when a mutant was serendipitously found to produce it (Harada et al., 1966). It was named after its ability to curdle, forming curd-like gels when heated in water. It was rapidly used as food additive for this property, since the end of the 1980's in Asia (McIntosh et al., 2005). This gel forming ability has been ascribed to a partial water solubility of native curdlan (Chen & Wang, 2020). In contrast, and although being composed of macromolecules with the same linear β-1,3 structure, paramylon granules extracted from euglenoids are completely insoluble in water and do not have such gel forming properties.

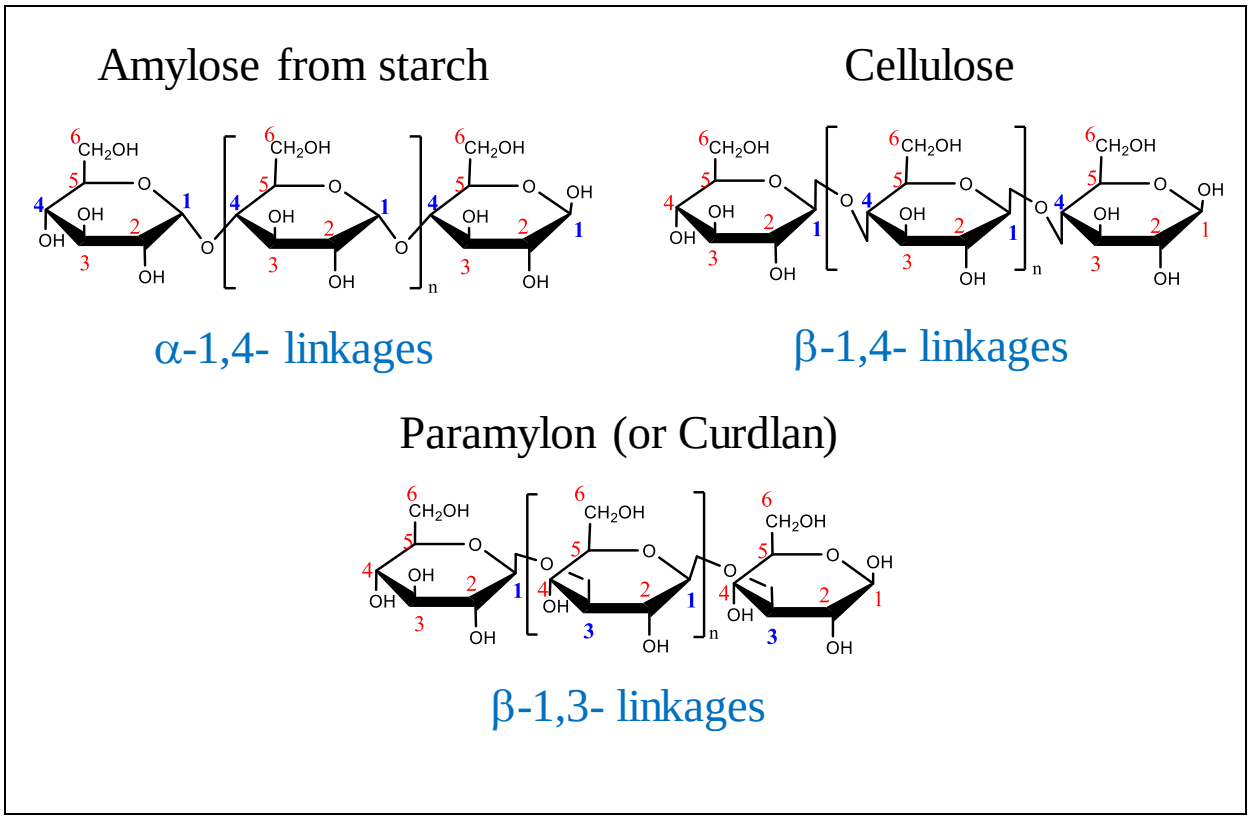

Figure 1: Macromolecular structure of linear glucans

Curdlan is found in various bacteria as an exopolysaccharide. It can be produced by fermentation with a high yield, and is easy to recover (McIntosh et al., 2005). Therefore, it has been produced industrially since the early 1990's. Registered by the Food and Drug Administration (FDA) in 1996, it remains mainly used as stabilizer, thickener, and texturizer in food, but also in pharmaceutical products. However, its unique biological activities are drawing more and more attention, as evidenced by a recent review article (Chen & Wang, 2020).

As an opposition, until the last decade, the cultivation of euglenoids, and consequently the production of paramylon, remained mostly confined to research laboratories. However, the present decade may see paramylon's development at industrial scale. Facilities for edible mass outdoor cultivation of *E. gracilis* exist in Japan since 2005. With the emergence of this microalga cultivation's industry, the research on paramylon has intensified more and more: If we consider the selected papers focused on paramylon cited in the present review, only 22 were

published between 1960 and 2010, while 57 papers were published in the last decade (20 for 2010-2015, 30 in 2015-2020, and already 7 papers in 2021).

Regarding potential applications, there has been a primary focus on food and health sectors. Paramylon was approved by the U.S. Food and Drug Administration in 2017 (*GRAS Notice for Paramylon Isolate from Euglena Gracilis*, 2017). A battery of toxicological studies was conducted on a dried preparation of *E. gracilis* biomass and pure paramylon to support their safe food use (Simon et al., 2016): it was shown that they are non-immunogenic and well tolerated (Del Cornò et al., 2020) when taken orally as food supplements. Generally speaking, the different biological activities of paramylon, and its resulting potential applications for health, are very similar to those of curdlan, which have been recently reviewed in detail (Chen & Wang, 2020). Along with remarkable anti-tumor (Quesada et al., 1976) and antimicrobial (Kottuparambil et al., 2019) properties, paramylon's alleged anti-inflammatory (Choi et al., 2013; Russo et al., 2017) and immunostimulatory activities are the most promising (Barsanti et al., 2011)**.** Paramylon granules effectively interact with pattern recognition receptors in animal and plant models (Barsanti & Gualtieri, 2019). The biopolymer was shown to promote the healing of epithelial wounds *in vitro*, and to suppress the acute inflammatory reaction caused by alkali burns in rats (Choi et al., 2013). Studies also showed a protecting role against acute liver damage induced by carbon tetrachloride (Sugiyama et al., 2009), and an inhibiting effect on the development of atopic dermatitis lesions in mice (Sugiyama et al., 2010).

The first available commercial products are dietary fibers based on unprocessed raw paramylon granules, or even raw *E. gracilis* biomass, as immune-stimulating agent (Skov et al., 2012; Kataoka et al., 2002). However, the specific role of paramylon remains unclear. A recent study suggest that it is not a potent imunomodulator by itself (Phillips et al., 2019), and that other molecules present in *E. gracilis* biomass and paramylon granules contribute to this bioactive property (Phillips et al., 2019).

In the present review, our final aim is to focus on the various processing routes leading to new potential paramylon based products, from nanofibers to biobased thermoplastics. However, we will start by briefly considering the cultivation of *E. gracilis* for the production of paramylon. Then we will take a closer look at the biopolymer's macromolecular structure, and to its crystallinity which is key for processing strategies. We will discuss the different paramylon solvents reported. Finally, the different processing routes, with and without chemical modification of the biopolymer, will be detailed together with the corresponding potential applications.

1) Paramylon production by cultivation of *Euglena gracilis*.

E. gracilis is a unicellular microalga belonging to the Euglenaceae family, or euglenoids, which is pervasive in nature. It is found in swimming pools, ponds, and most freshwater, or brackish biotopes. Contrary to bacteria, euglenoids do not present any pathological risk to humans. *E. gracilis* can be safely grown in large quantities by different ways including photoautotrophic (using sunlight and CO_2), heterotrophic (using an external organic carbon source) or a combination of both (Rodríguez-Zavala et al., 2010; Grimm et al., 2015).

In general, microalgae are an important potential source of metabolites including polysaccharides, proteins, lipids and pigments. In the case of *E. gracilis*, various metabolites of interest such as dietary proteins, lipids, wax esters, tocopherol, carotenoids, and paramylon can be produced, as highlighted in various recent review articles (Gissibl et al., 2019; Kottuparambil et al., 2019). Paramylon is the unique reserve polysaccharide of the microalga. It is found in proportion ranging from 50 to 80% of the cell's dry weight (Watanabe et al., 2013). Other euglenoids such as *Euglena cantabrica* also contain paramylon, with similar content from 34 to 80% (Muñóz-Almagro et al., 2020).

The robustness and versatility of *E. gracilis* allow the production of paramylon within the framework of environmental-friendly schemes (bioremediation, wastewater treatment, CO_2 trapping …), taking advantage of the various trophic conditions depending on the available resources (light, carbon …): euglenoids can grow with a remarkably high tolerance to stressful environments: They are acidophilic and can tolerate high concentrations in heavy metals. Therefore, they may be used for bioremediation of contaminated waters (Krajčovič et al., 2015), while producing valuable metabolites, including paramylon. The heterotrophic cultivation of *E. gracilis* can involve nutrients recovered from wastewater (Aida et al., 2016; Rubiyatno et al., 2021): For example, the hydrothermal conversion of solid sludge residues lead to ammonia and phosphoric acid rich culture media allowing higher growth rates than a standard AF-6 culture medium. The authors pointed out the high tolerance of *E. gracilis* to ammonia, which concentration was ten times higher than in AF-6 medium (Aida et al., 2016).

One typical problem with heterotrophic microalgae cultivation is the noxious proliferation of bacteria. However, in the case of *E. gracilis*, this can be beneficial to paramylon productity: Co-cultivation with bacteria *Pseudoalteromonas* in heterotrophic conditions (Jeon et al., 2020) can increase paramylon yield by 34%. Last but not least, due to its fast growing acidophilic nature, *E. gracilis* is particularly interesting for the direct conversion of CO_2 into biomass (Piiparinen et al., 2018). The gas can be directly injected in the liquid cultivation media. The resulting decrease of pH is beneficial to the specific growth rate (SPR) of the microalga. Maximum SPR values of 0.9 per day are reported at pH 3 under continuous light, with a considerable CO_2 consumption of about 2.4 g per g of biomass (Piiparinen et al., 2018).

This makes paramylon a potentially carbon neutral biopolymer. The storage polysaccharide is produced by *E. gracilis* in autotrophic, heterotrophic or mixotrophic conditions (Krajčovič et al., 2015). However, aerobic conditions are required. Anaerobic conditions lead to different storage molecules such as wax esters, myristic acid being the main component (Inui et al.,

1983). It is indeed possible to induce the conversion of wax esters to paramylon by switching form anaerobic to aerobic conditions (and vice versa). **Table 1** sums up the impact of the *E. gracilis* cultivation conditions on the paramylon dry weight content of microalga biomass. Photoautotrophic conditions lead to the lowest values: 20 % or lower depending on light intensity and duration of cultivation (Grimm et al., 2015; Cook, 1963) because, as a storage polysaccharide, its biosynthesis in photoautotrophic conditions only corresponds to excess energy (Grimm et al., 2015). Therefore, paramylon content can be enhanced by increasing light intensity (Cook, 1963): For low intensities, protein production is predominant, while for very high light intensities, paramylon content becomes higher. However, such photoautotrophic conditions should be used only if no organic carbon source is available, or if one wants to avoid the cost of such nutrients.

When cheap nutrients are available, such as biomass waste (Aida et al., 2016), heterotrophic conditions are generally more interesting. Indeed, as shown on **Table1**, higher paramylon content can be obtained in purely heterotrophic conditions (50-80% paramylon with an organic carbon source, in absence of light and CO_2). In presence of light, the paramylon content tends to be lower, either for purely photo-heterotrophic conditions (with an organic carbon source, in absence CO_2) (Matsuda et al., 2011), or for mixotrophic conditions (with an organic carbon source and CO_2) (Grimm et al., 2015). However, this concentration greatly depends on the duration of the cultivation because the accumulation of paramylon continues during the stationary phase (Grimm et al., 2015). Paramylon contents of 50% after 7 days have been recently reported for mixotrophic cultivation using sewage effluents as cultivation media opening the perspective of transforming wastewater treatment plants into sustainable paramylon production facilities (Rubiyatno et al., 2021). Note that the data in **Table 1** concerns only wild type *E. gracilis* strains. Mutant strains were reported to accumulate up to 90% of paramylon when grown in the dark, with an adequate carbon source (Barsanti et al., 2001). It

should also be noted that cultivation strategies can also be developed in order to optimize the coproduction of paramylon and other metabolites of interest: For example α-Tocopherol which requires light. In such a case, mixotrophic conditions offer a better compromise than purely heterotrophic ones (Grimm et al., 2015).

Table 1: Influence of *Euglena gracilis*'s cultivation conditions on the paramylon dry weight content of microalga biomass.

Cultivation conditions			**Cultivation days**	**Paramylon content (%)**	**Ref.**
Aerobic	Light (continuous)	Photo-autotrophic 1000 μmol.m^{-2}.s^{-1}	4	10	(Grimm et al., 2015)
			7-10	23	
		Photo-heterotrophic 108 μmol.m^{-2}.s^{-1}	3	33	(Matsuda et al., 2011)
		Mixotrophic 1000 μmol.m^{-2}.s^{-1}	7	40	(Grimm et al., 2015)
			10	72	
	Darkness	Heterotrophic	3	58	(Matsuda et al., 2011)
			7	75	(Grimm et al., 2015)
			10	83	(Grimm et al., 2015)
Anaerobic	Light or darkness	Photo-heterotophic or heterotherophic	Wax esters (no paramylon)		(Krajčovič et al., 2015)

In early studies, authors remarked that paramylon is found in the cells as microscopic granules, insoluble in water, and highly resistant to chemical or enzymatic attack, except for very specific enzymes (Meeuse, 1964). Thus, rather than solubilizing the biopolymer, it can be recovered in its native granular state. This requires disrupting the cells and eliminating the other metabolites which are mostly lipids, pigments and proteins. Paramylon granules can then be recovered by centrifugation, before being dried (Clarke & Stone, 1960) or freeze-dried (Kobayashi et al., 2010). This extraction process can be applied to fresh *E. gracilis* biomass (Zhong et al., 2021) or previously lyophilized biomass (Tanaka et al., 2017). However, there is no standard method. The exact nature of the different steps, and the order in which they are performed, varies from one author to another:

- The most common cell disruption method is mechanical. It typically involves sonication in an aqueous medium where the biomass is dispersed (Tanaka et al., 2017). However, enzymatic cell dissociation using trypsin has also been reported (Grimm et al., 2015) though it seems rather used for quantification of paramylon content, rather than for bulk extraction.
- Hydrophobic compounds (lipids and pigments) are usually removed using polar solvents. Acetone or ethanol are the most widely used, but other solvents such as chloroform or chloroform/ethanol mixtures have been reported (Clarke & Stone, 1960).
- Protein extraction can be done using detergents such as sodium dodecyl sulfate or sodium lauryl sulfate, either at low temperature for a relatively long time (e.g. 24 hours at 20-40°C) or at higher temperature with shorter times (e.g. 30 minutes at 70-100 °C) (Tanaka et al., 2017; Kobayashi et al., 2010).

Such paramylon granules extraction methods are also used to monitor microalga cell's paramylon content during cultivation (Šantek et al., 2012; Grimm et al., 2015). However, as they require several steps and hours, more sophisticated techniques have been developed: Real-

188 time direct quantification of the intracellular components at the single cell resolution has been
189 reported (Wakisaka et al., 2016). However, a potentially cheaper and less-than-one-hour-long
190 alternative consists in disrupting the cells, and using specific fluorescent DNA aptamers having
191 a binding affinity with paramylon granules (Kim et al., 2020) for their quantification.

192 **2) Macromolecular and crystalline structure of paramylon**

193 In this section, we will see how paramylon is structured at different scales starting from the
194 macromolecular structure of the biopolymer up to the granules. The various differences with
195 curdlan will be discussed.

196 The macromolecular structure of paramylon is generally presented as perfectly linear, with only
197 β-1,3 linkages between glucosidic repeating units (Stone, 2009). However, according to a recent
198 report of the US Food and Drug Administration (*GRAS Notice for Paramylon Isolate from*
199 *Euglena Gracilis*, 2017), a detailed analysis shows that the β-1,3 linkages content is closer to
200 94%. The other linkages identified are mostly β-1,4 and β-2,3 linkages, each in the 2 to 3 %
201 range. Therefore, small "defects" are present in paramylon's linear macromolecular
202 architecture. The same applies for curdlan, but with different "defects" since it is known to
203 contain few β-1,6 linkages (McIntosh et al., 2005).

204 The size of curdlan and paramylon macromolecules are also significantly different. The
205 reported average molecular weight for paramylon is typically between 100 and 500 kDa
206 (Koizumi et al., 1993; Barsanti et al., 2011), which corresponds to a number of glucose units
207 between 600 and 3000. This value is about 4 times lower than for curdlan, for which molecular
208 weights of 2000 kDa (≈12000 glucose units) have been measured by viscosimetric
209 measurements (Futatsuyama et al., 1999). More recent measurements by size-exclusion
210 chromatography with multi-angle laser-light scattering method confirmed the ratio of
211 approximately 4 between the average molecular weights of paramylon and curdlan (Tamura et

al., 2009). However, number and weight average number of glucosidic units obtained by this technique were about half of those obtained by viscosimetric measurements (Tamura et al., 2009).

Last but not least, paramylon strongly differs from curdlan in terms of native crystallinity. A crystallinity index of approximately 88% was estimated for paramylon granules from density measurements, compared to only 30% for native curdlan (Marchessault & Deslandes, 1979). Moreover, the native crystalline structures of the two biopolymers are fundamentally different, despite they both involve a parallel arrangement of the chains, that take different helical conformations: Native paramylon only involves highly stable and water insoluble triple helices conformers, while native curdlan microfibrils also involve less stable, and water-soluble, single helices conformers (Chen & Wang, 2020). This explains why, unlike paramylon, curdlan is partially water-soluble, the later rearrangements of the chains and microfibrils leading to gelation (Chen & Wang, 2020).

The native crystalline arrangement of the helices is also different: In native curdlan, the simple helices are arranged in orthorhombic crystalline cells (Okuyama et al., 1991), while in paramylon the triple helices are arranged in hexagonal crystalline cells (Marchessault & Deslandes, 1979; Chuah et al., 1983). It has to be noted that this difference was not clear until the early 1990's (Okuyama et al., 1991) because the X-Ray Diffraction early studies did not involve native curdlan, but recrystallized samples. Indeed, such recrystallized curdlan adopts the same triple helices/hexagonal structure as paramylon (Marchessault & Deslandes, 1979; Marchessault et al., 1977).

Figure 2, drawn after (Marchessault & Deslandes, 1979) and (Chuah et al., 1983), gives a closer look at this multi scale crystalline structure of paramylon:

- At the lower scale, groups of 3 chains are assembled forming a triple helix (6/1 right handed (Chuah et al., 1983) with an advance of approximately 2.9 Angstrom per

monomer unit (Marchessault et al., 1977).) These triple helix structural units are very stable, mostly due to internal hydrogen bonds that involve only the C2 secondary hydroxyl groups of each glucosidic unit (Chuah et al., 1983). These bonds are assumed to form a hexagonal shape perpendicular to the helix axis (as shown with dotted line on **figure 2**). However, according to an alternative model, other hydrogen bonds not perpendicular to the axis may involve secondary C2 OH groups in different x,y planes (Miyoshi et al., 2004). This alternative model is theoretically more stable for β-1,3-glucans containing more than ten glucosidic units (Miyoshi et al., 2004).

- Parallel triple helices then form the hydrogen bonded hexagonal crystalline structure (Deslandes et al., 1980). The dimensions of the hexagonal unit cell depend on moisture content. Only paramylon occurs in the (almost fully) dry high density form, while water molecules are always present in the unit cell for recrystallized curdlan (Marchessault & Deslandes, 1979; Chuah et al., 1983).

The transition between dry and hydrated polymorphs of paramylon is reversible with a large hysteresis: upon drying, the transition from hydrated to dry polymorph takes place around 30% relative humidity, and around 70% relative humidity the other way round (Kobayashi et al., 2010). One molecule of water per glucopyranoside residue is present in the hydrated form for which the in-plane dimensions are a = b = 15.56 Å, while c = 18.78 Å is equal to the repeating length of the triple helices (Deslandes et al., 1980). Upon drying, the dimensions of the cell are shrunk to a = b = 14.41 Å and c = 5.87 Å (Chuah et al., 1983), so that this later corresponds to 1/3 of the repeating length of the triple helices. Such a transition to the dry polymorph can also occur upon heating due to water evaporation, therefore impeding any possibility for the melting of the crystalline structure, without thermal degradation of the biopolymer, as shown by recent hot compression molding experiments on paramylon and curdlan (Kawahara et al., 2020).

The paramylon granules can have different shapes depending on the euglenoid strain. At least six different morphological variations have been reported, from disks to rods (Monfils et al., 2011). For *E. gracilis*, the shape is typically flat cylindrical with reported diameters around 5µm and thicknesses about 3 µm (Anraku et al., 2020). The granules are actually surrounded by a biomembrane. Inside these paramylon native granules, schematically represented on **Figure 2**, the triple helices are arranged tangentially, while curdlan have a more spherulite-like microstructure (Marchessault & Deslandes, 1979). It is assumed that paramylon is first biosynthesized as elementary microfibrils with low crystallinity (Kiss et al., 1987, 1988): as the granule matures, the microfibrils assemble to form the final highly ordered crystalline structure with concentric deposition of aggregates of elemental nanofibers of 4-10 nm. Recently, morphometric characterizations by focused ion beam/scanning electron microscopy (FIB/SEM) tomography (Anraku et al., 2020) confirmed that the paramylon particles have a very dense structure without large void spaces. A specific surface area (SSA) of 2.438 m^2/g was measured by BET which is close to starch granules from potatoes and corn.

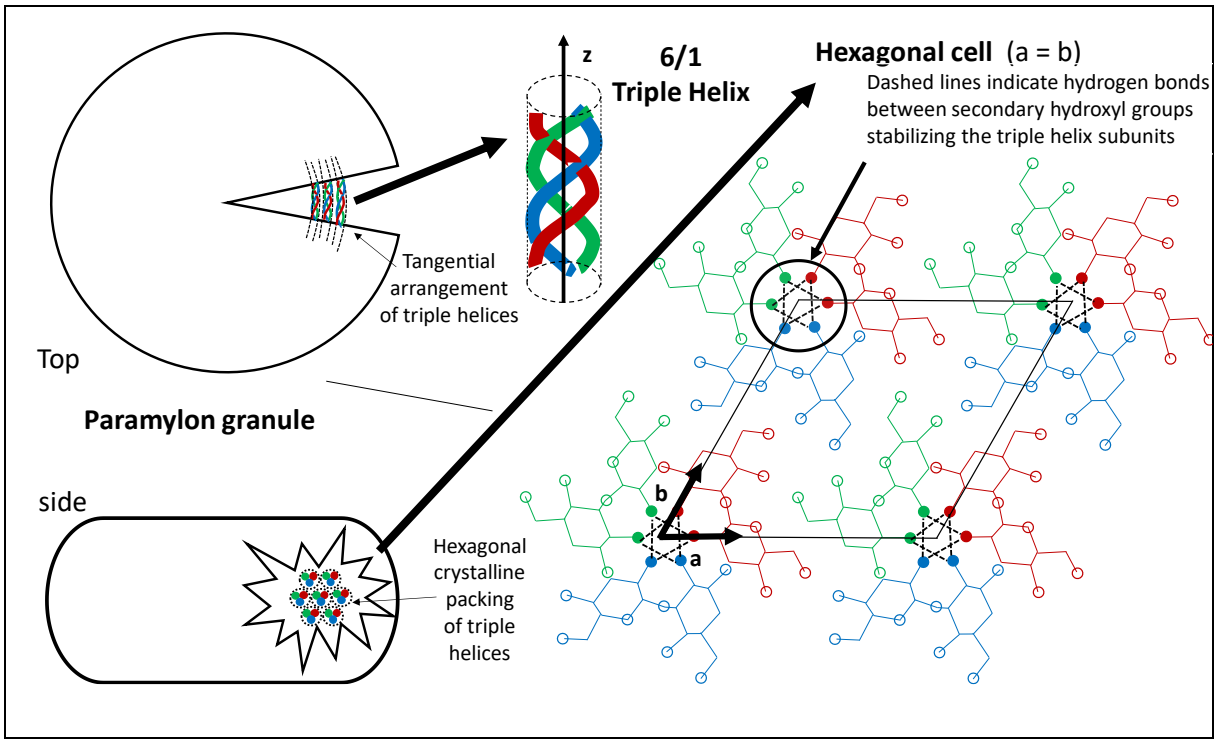

Figure 2: Multiscale structure of native paramylon.

Summing up, paramylon is similar to curdlan but presents structural differences at different scales, from the "defects" present at the macromolecular structure level of the chains, to the native crystalline arrangement. However, the key difference is probably the presence of water-soluble single-helices in curdlan, explaining its gel forming properties, while paramylon is completely water insoluble. Therefore, the processing of paramylon into materials requires the use of specific solvents and/or chemical modifications.

3) Solvents of paramylon

Like cellulose or starch, paramylon is water insoluble and has very few known solvents. This limited solubility can be explained not only by the stability of the crystalline structure which is extensively hydrogen bonded (Deslandes et al., 1980) but also, and mostly, by the stability of the individual triple helices, due to the intermolecular hydrogen bonds between C2 secondary OH groups (Chuah et al., 1983) (**Figure 2**). Indeed, some of the oldest known and most frequently used solvents of paramylon are alkaline aqueous solutions (NaOH (Clarke & Stone, 1960; Manners et al., 1966) or KOH (Vogel & Barber, 1968)). They can dissolve the biopolymer either "completely" in the form of random coils, or "partially" as individual triple helices, depending on the alkaline concentration: In dilute alkaline solutions, paramylon granules are disrupted into elemental 4 nm microfibrils (Kiss et al., 1988). Triple helices disrupt for NaOH concentrations higher than 0.22 M. This transition can be detected by adding Congo Red to the solution since the dye forms a complex with the triple helices (Shibakami et al., 2013a). Note that such a triple helix to random coil transition at extreme pH is reversible upon lowering alkaline concentration. For paramylon the reverse random coil to triple helices transition takes place for NaOH concentrations around 0.17–0.20 M allowing the formation of nanofibers by self-assembly (Shibakami et al., 2013a).

Concentrated NaOH solutions are also used as a medium for homogeneous chemical modification of paramylon (Daglio et al., 2019; Shibakami et al., 2016) and for purification of

paramylon by solubilization and precipitation by addition of ethanol (Russo et al., 2017). Recently, aqueous solutions of curdlan in various states from triple helices to random coils and intermediate state were obtained by first solubilizing the biopolymer in NaOH solutions followed by neutralization with HCl solutions of the same concentration (Yan et al., 2020). This approach can also be applied to paramylon. Indeed, a Japanese patent application from 2011 (Arashida et al., 2011) describes the preparation of "amorphous" paramylon (actually partially recrystallized as single helices) by a similar solubilization/neutralization process. This process leads to a low apparent density paramylon powder (0.1g.cm^{-3}) with significantly increased water and oil absorption performances compared to raw paramylon granules, improving potential benefits as dietary fibers (Arashida et al., 2011).

Other reported solvents of paramylon working at room temperature are listed in **Table 2**. Formaldehyde and **c**oncentrated acids, such as H_2SO_4 (55%) and anhydrous formic acid, were reported as solvents in early studies (Clarke & Stone, 1960). Formic acid was later used for production of films by evaporation casting despite it has the drawback of depolymerising paramylon by acid hydrolysis (Clarke & Stone, 1960; Kawahara & Koganemaru, 2006). Moreover, for acidic solvents there seem to be no evidence in literature that the triple helices are disrupted.

Some solvents able to destabilize hydrogen bonds allow disrupting the triple helices structure, in particular dimethylsulfoxide (DMSO): It has been used for producing oriented curdlan fibers for XRD studies by dissolution and coagulation in methanol (Chuah et al., 1983) and to obtain paramylon single helices by solubilisation followed by lyophilisation of the DMSO solution (Aketagawa et al., 1993). However, DMSO is essentially used for viscosimetric measurements, for which it is preferred to NaOH solutions. For this latter, a study with curdlan samples of various molecular weights (including small molecular weights comparable to that of paramylon) showed that the viscosity strongly depends on the alkaline concentration, and the

resulting state of the macromolecules (random coils or triple helices) (Futatsuyama et al., 1999). As an opposition, macromolecules are always in the form of random coils in DMSO (Futatsuyama et al., 1999), resulting in viscosities that depend only on curdlan concentration, molecular weight, and temperature. Therefore, the Mark-Houwink parameters have been determined for curdlan in DMSO at 25°C (Futatsuyama et al., 1999) allowing the determination of the average molecular weight by viscosimetry. This method has also been applied to paramylon molecular weight evaluation (Kawahara & Koganemaru, 2006). Note that mixtures of water with cadoxen (cadmium and ethylenediamine based solvent) have been also reported as efficient solvents of curdlan (Futatsuyama et al., 1999) for viscosimetric measurements and so may be used also for paramylon. However the authors recommend to use DMSO (Futatsuyama et al., 1999)."

More precise measurements can be made using SEC/MALLS technique using a mixture of 1% LiCl in 1,3-Dimethyl-2-imidazolidinone (DMI) as eluent (Tamura et al., 2009). DMI/LiCl is indeed an efficient solvent of both curdlan and paramylon, but requires heating at 100°C. Dimethylformamide (DMF)/ LiCl has also been recently reported as a solvent for paramylon homogeneous modification at 70°C (Seok et al., 2021)

The other reported hydrogen bonding solvents, listed in **Table 2,** also require heating in order to completely dissolve paramylon. N,N-Dimethylacetamide with a small amount of lithium chloride (typically DMAc/ LiCl 8g.l^{-1}) has been used as an efficient media for homogeneous chemical modification (Shibakami, 2017; Shibakami et al., 2014). Recently, a mixture of DMAc with and ionic liquid (1-butyl-3-methylimidazolium chloride) with a [Bmim][Cl]/DMAc volume ratio of 5:2 was used as a solvent of paramylon (Yasuda et al., 2018). No details are given about the state of the paramylon molecules in the solution. However, recent works on the solubility of curdlan in another imidazolium ionic liquid (1-ethyl-3-methylimidazolium acetate ([Emim][OAc])) suggest complete solubility as random coils (Bai

et al., 2019). Therefore, ionic liquids may be a new family of solvent for paramylon. Nevertheless, depolymerization may be an issue: significant molecular mass decrease was observed for curdlan after 2 hours at 80°C in [Emim][OAc] (Suzuki et al., 2021).

Summing up, due to its crystalline structure and its triple helix conformation (stabilized by interchain hydrogen bonds involving the C4/C6 –OH groups, and the C2-OH groups, respectively), paramylon is only soluble at extreme pH (acidic or basic) or in solvents able to form strong hydrogen bonds. Moreover, its solubility can be either complete, with individual paramylon macromolecules taking a random coil conformation, or partial with remaining triple helices, depending on the ability of the solvent to completely or partially disrupt the different interchain hydrogen bonds.

362 **Table 2**: Solvents of paramylon reported in literature; with their respective known drawbacks and applications.

Solvent	State of macromolecules	Known drawback	Main applications	References
Formaldehyde	unknown	toxicity	none	(Clarke & Stone, 1960)
DMSO	random coil	none	viscosimetry	(Futatsuyama et al., 1999) (Kawahara & Koganemaru, 2006)
			recrystallization of paramylon monohelices	(Aketagawa et al., 1993).
KOH	unknown	unknown	none	(Vogel & Barber, 1968)
NaOH < 0.22 M	triple helix	incomplete solubilization	extraction	(Clarke & Stone, 1960; Manners et al., 1966)
			fractionation into microfibrills	(Kiss et al., 1988)
			Self-assembly	(Shibakami et al., 2013a)
NaOH > 0.22 M	random coil	None	purification,	(Russo et al., 2017)
			"amorphisation"	(Arashida et al., 2011)
			chemical modification	(Daglio et al., 2019; Shibakami et al., 2016)

H_2SO_4 (55%)	unknown	depolymerization	none	(Clarke & Stone, 1960)
Formic acid (90%)	unknown	depolymerization	solvent casting	(Kawahara & Koganemaru, 2006)
DMAc / LiCl	random coil	temperature (≈ 100°C)	chemical modification	(Shibakami et al., 2014)
BMIMCl/ DMAc	unknown	temperature (60-70°C)	film regeneration	(Yasuda et al., 2018)
BMI/LiCl	random coil	temperature (≈ 100°C)	chromatography	(Tamura et al., 2009)
DMF/LiCl	random coil	temperature (≈ 70°C)	chemical modification	(Seok et al., 2021)

363

4) Processing of paramylon without chemical modification

The preservation of paramylon's unique β-(1,3) linear macromolecular structure allows targeting applications as materials that take advantage of two intrinsic properties: the biological activity, and the mechanical properties induced by its triple helix based crystallinity. According to some authors, the synergistic optimization of these properties may however be difficult to achieve since biological activity tends to be enhanced by an amorphous structure, while mechanical reinforcement requires a high crystallinity (Kawahara, 2014).

Almost all the processes described in the scientific and patent literature involve at least two steps: First, native paramylon granules (or previously purified paramylon powder) is solubilized. Then in a second step, paramylon is regenerated in the targeted shape (powder, fibers, films) by elimination of the solvent, either by evaporation when it is volatile or by washing with a non-solvent of paramylon. However, in a recent study solvent free processing of paramylon and curdlan was intended: Both polymers were hot pressed into films at temperatures around 200°C, with optimal conditions around 220 and 230°C for paramylon and curdlan, respectively (Kawahara et al., 2020). However, the XRD data suggest that the crystalline structure never completely melts. The persistence of some peaks and the appearance of new ones at high temperatures rather suggest rearrangements, which differ between curdlan and paramylon samples. In addition, significant degradation and subsequent uncontrolled crosslinking reaction occur. However, this hot press process leads to materials with mechanical properties comparable to those of Polyamide 12 in terms of flexural modulus and strength, and to those of epoxy resins in terms of elongation at break (Kawahara et al., 2020).

In 2006, Kawahara & Koganemaru (Kawahara & Koganemaru, 2006) were the first to show the feasibility of film casting from paramylon solutions in 90% formic acid. Transparent/yellow films were obtained by slow evaporation of the solvent. X-ray diffraction and tensile tests indicated that the films were mostly amorphous with glassy behaviour (Young's modulus ≈ 1

GPa and elongation at break < 15%). Partial recrystallization was observed by annealing under water steam, leading to higher stiffness and lower elongation. A decrease of films mechanical properties was observed for very long residence time in formic acid solution (> 72 hours) before film casting. It was ascribed to depolymerisation hydrolysis, leading to paramylon oligomers, as confirmed by viscosimetric measurements (Kawahara & Koganemaru, 2006). The same authors tried, without success, to produce paramylon fibers by wet spinning using a solution of Na_2SO_4 as coagulation bath. Blending with polyvinyl acetate (PVA) (initially co solubilized in formic acid) improved the spinnability, but resulted in low mechanical properties due to incompatibility of the PVA/paramylon mixture (Kawahara & Koganemaru, 2006).

Formic acid was also used as a co-solvent of paramylon and silk fibroin for the preparation of blend films (Arthe et al., 2020)**.** Despite, the high hydrophobicity of the protein, the blends obtained seemed to be compatible, according to AFM and SEM observations showing no heterogeneities at the micrometre scale. Infrared spectroscopy did not show specific interactions between the biopolymers. However, a synergy was observed in terms of mechanical properties: for a 75:25 protein:paramylon ratio, the stiffness of the blend films was twice higher than that of the pure biopolymers films (Arthe et al., 2020). The authors showed that the blends present a combination of properties (low water absorption/swelling capacity, blood compatibility and non-toxicity) suitable for wound healing applications. This kind of potential application was also reported for pure paramylon 20-µm thick films produced using a [Bmim][Cl]/DMAc mixture as a solvent (Yasuda et al., 2018). Due to the non-volatility of the ionic liquid, the regeneration of paramylon films required washing with a non-solvent (methanol) and drying. Unfortunately, no characterization of the films' structure and mechanical properties are provided. Only their biological activity is investigated, showing wound healing properties by inhibiting inflammatory aggression, suggesting potential wound dressing applications (Yasuda et al., 2018).

Regarding the shaping of fibers, it can be first recalled that curdlan was shaped as oriented fibers for XRD studies, by solubilisation in DMSO and coagulation in methanol (Chuah et al., 1983). More recently, curdlan was shaped into fibers by wet spinning from solutions in 1-ethyl-3-methylimidazolium ionic liquid [Emim][OAc] (Suzuki et al., 2021)**.** The authors reported a solubility of curdlan up to 9 wt.% in the ionic liquid at 80°C. The dope was extruded in air and spin drawn in two different coagulating baths (water or ethanol). For optimized spinning conditions, the semi-crystalline transparent fibers obtained combined relatively high Young's modulus (≈ 2 GPa) and high elongation at break (up to 40%). A similar processing route may be applied for the production of paramylon fibers. However, the authors reported a significant decrease of the molecular mass of curdlan, which was almost divided by two. This suggest a depolymerisation of the biopolymer while in solution in the ionic liquid. In the case of paramylon which already has much lower molecular masses than curdlan, this may be an issue.

Paramylon nanofibers can be obtained by two methods : electrospinning (Kawahara, 2014) and self-assembly (Shibakami et al., 2013a): Fully amorphous paramylon nanofibers were obtained by electrospinning of paramylon solutions in formic acid. In this work the author takes advantage of the unavoidable hydrolysis kinetics of paramylon by formic acid to optimize the viscosity of the solution so that the appropriate range of Berry number (i.e. intrinsic viscosity × concentration) for electrospinning is matched. The nanofibers obtained had diameters ranging from 50 to 500 nm (average value 192 ± 135 nm). Being fully amorphous, they were too brittle for mechanical reinforcement. However, the author proposed to use them for the production of biologically active amorphous micropowder by grinding (Kawahara, 2014).

A different approach for the production of crystalline nanofibers is a bottom up approach taking advantage of the intrinsic self-assembly behaviour of β-1,3-glucan chains (Shibakami et al., 2013a) . This ability had been previously described for other β-1,3-glucans with pendant chains such as schizophyllan (Sletmoen & Stokke, 2008), but its application to nanofibers production

is only possible with paramylon chains, which do not present branching. Indeed, the control of alkaline solvent NaOH concentration allows triggering the transition of paramylon solubilized macromolecules from individual random coil, at high concentration, to triple helix rods, when the NaOH concentration is decreased. Thus for linear chains, large nanofibers can be obtained apparently consisting of more than 100 triple helices (Shibakami et al., 2013a). It is striking that these large nanofibers seem to be constituted of smaller 4 nm nanofibers which is the size of elemental nanofibrils reported when paramylon granules are disrupted in dilute alkaline solutions (Kiss et al., 1988). Moreover, it has to be noted that, as shown on **Figure 2,** the formation of triple helix and its stabilisation by internal hydrogen bonds involves only the C2 secondary hydroxyl groups of each glucosidic unit (Chuah et al., 1983). Consequently, the remaining hydroxyl groups, which are external to the helices, can be chemically modified without losing the self-assembly properties (Shibakami et al., 2013b). Unmodified paramylon nanofibers prepared by such a self-assembly approach showed an anti-fibrotic effect on liver damage induced by carbon tetrachloride (Kusmic et al., 2018). These 10 nm thick nanofibers were efficient at a dosage about 20 times lower than in previous studies involving paramylon granules (Sugiyama et al., 2009). Nanofibers also effectively interact with pattern recognition receptors in animal and plant models (Barsanti & Gualtieri, 2019).

The above literature results demonstrate that is it possible to use solvent based processes in order to transform native paramylon granules into different shapes (powder, films, fibers and nanofibers) and blends with other polymers, while preserving its native chemical structure (only the molecular weight is decreased in some cases). This solvent based processing also allows modifying the physical structure of paramylon chains, which can become partially or completely amorphous. However, when mechanical properties were characterized, amorphous structures tend to result in brittleness, both for nanofibers and films. In addition, the available data does not allow evidencing a relationship between an amorphous structure and enhanced

bioactive properties. Indeed, for nanofibers (the only shape for which both fully amorphous and highly crystalline structures are reported), the bioactive properties of electrospun amorphous nanofibers were not characterized, while crystalline self-assembled nanofibers showed improved bioactivity compared to native paramylon granules.

Concurrently, solvent free processing trials by hot press up to 230°C showed that paramylon is not thermoplastic. Indeed, despite semi-crystalline films with mechanical properties comparable to engineering polymers could be obtained by this process, this was not possible without simultaneous thermal degradation and uncontrolled crosslinking. The absence of melting of paramylon's crystalline structure below its degradation temperature may be related to the shrinkage of the hexagonal cell upon drying, which is likely to make it more stable upon heating, thus preventing melting.

5) Chemical modifications of paramylon

Each sugar residue of β-1,3-glucan chains presents three hydroxyl groups that can be used as modification sites located the C2, C4 and C6 carbons (**Figure 1**). The primary C6 -OH group is more reactive (Chen & Wang, 2020). The various chemical modifications reported in literature are either non-selective or regioselective. They are conducted either in homogeneous conditions, using some of the solvents listed in **Table 2**, or in heterogeneous conditions after dispersion of paramylon in non-solvents. The two main kinds of modified paramylons described in literature are ionic derivatives (paramylon sulfates, salts of paramylon ethers and one salt of paramylon acid) (**Table 3** and **Table 4**), and different types of paramylon esters and mixed esters (including some bearing an ionic group) (**Table 4** and **Table 5**).

However, before focusing on these two main categories, we have to mention a recent alternative approach, in which crosslinked hydrogels were obtained by reacting paramylon and curdlan with ethylene glycol diglycidyl ether (EGDGE) (Matsumoto et al., 2021). The reaction between

488 the epoxy functions of the crosslinker and the hydroxyl groups of the biopolymers was
489 performed in a 1M NaOH aqueous solution at room temperature during 48 hours. After
490 neutralization with acetic acid and washing with water, self-standing gels were obtained. The
491 authors tested different initial paramylon concentrations and varied the polysaccharide:EGDGE
492 ratio. Though the crosslinking efficiency was rather low, with a maximum of 43% of the initial
493 EGDGE content present in the hydrogels, the hydrogels showed high deformability in
494 compression, up to 94% strain at break, and remarkable shape recovery when deformed at 80%
495 strain. However, the shape recovery for hydrogels obtained by crosslinking of paramylon was
496 lower than that of curdlan based hydrogels. In addition, a higher initial concentration of
497 polysaccharide is required in the case of paramylon. These results were ascribed to the higher
498 molecular weight of curdlan, leading to entanglements even at low concentrations (Matsumoto
499 et al., 2021). It should be pointed out that the same research group produced curdlan based
500 organogels by subsequent acetylation of crosslinked hydrogels (Enomoto-Rogers et al., 2016).
501 These organogels were hydrophobic and swell in chloroform. The same approach could
502 potentially be applied to crosslinked paramylon.

503 **5.1) Paramylon sulftate, ether, and acid ionic derivatives**

504 The various reported anionic and cationic paramylon derivatives (except esters) obtained by
505 homogeneous and heterogeneous reactions are listed in **Table 3**. To our knowledge the first
506 reported modified paramylons are anionic and cationic derivatives (Koizumi et al., 1993). The
507 authors report a significant increase of water solubility of all the ionic derivatives, which results
508 in an inhibitory activity against human immunodeficiency virus (HIV) for sulfated paramylon
509 with a sulphur content above 4%. The highest anti-HIV activities were obtained for sulphur
510 contents in the 12.6% to 14.0% range (Koizumi et al., 1993), which corresponds to values of
511 degree of substitution (DS) between 1.2 and 1.7. However, the authors do not give information
512 about the chemical modification conditions. Similar properties were previously reported for

sulfated curdlan (Yoshida et al., 1990). The homogeneous modification of curdlan was performed in solution in DMSO, by reaction with piperidine-N-sulfonic acid. The DS values ranged from 0.8 to a maximum of 1.6 (100% for C6, ≈5% for C4 and 40% for C2) (Yoshida et al., 1990). Given that paramylon is also soluble in DMSO and presents the same macromolecular structure as curdlan (with shorter chains), we assume that similar non-regioselective sulfatation reaction conditions can be applied to paramylon. However, we do not know if this was the case in the work on sulfated paramylon (Koizumi et al., 1993).

More recently, anionic paramylon ether derivatives were obtained by carboxymethylation, leading to sodium salts of carboxymethyl paramylons that are not only water-soluble, but also showed nanofiber forming ability (Shibakami et al., 2016). The modification was performed both in homogeneous and heterogeneous conditions. Homogenous reaction with chloroacetic acid in concentrated NaOH leads to low DS ≈ 0.13. Note that slightly higher DS ≈ 0.25 were obtained in the same homogeneous conditions by other authors who suggest applications as pharmaceutical tablets disintegrant (Daglio et al., 2019).

Heterogeneous carboxymethylation in a mixture of 2-propanol and NaOH aqueous solution allowed a better control of the DS with values ranging from as low as 0.015 up to 0.78 (Shibakami et al., 2016). However, this heterogeneous reaction required the previous preparation of "amorphous" paramylon by solubilisation in NaOH aqueous solution followed by neutralization with HCl as described in a patent application from 2011 (Arashida et al., 2011). The nanofiber forming ability depends on the DS range: For $0.07 < DS < 0.78$, the nanofiber forming was observed in solution in water, whereas for lower $0.015 < DS < 0.07$, a nanofiber gel is formed in water, leading to aerogels maintaining their fibrous structure when freeze-dried. (Shibakami et al., 2016). The formation mechanism of these nanofibers was not investigated but involves previously water solubilized chains. Therefore, it is probably similar

to the self-assembly mechanism described by the same group for non-derivatized paramylon (Shibakami et al., 2013a).

Anionic paramylon acid derivatives were also obtained by regioselective heterogeneous oxidation of C6 -OH groups, mediated with 2,2,6,6-tetramethylpiperidine-1-oxyl radical (TEMPO) in water at pH 10 with NaBr and NaClO (Tamura et al., 2009). Up to 100% substitution of C6-OH groups was observed. The resulting (1→3)-β-D-polyglucuronic acid sodium salt was water-soluble. However, this was not the case for the other lower DS values studied (1% to 43% substitution of C6-OH groups) which remained insoluble in water, pointing out the need for a minimum degree of such regioselective substitution for water solubility. This contrast with the anionic ether paramylon derivatives may be due to the acid linkage. The C2 secondary OH groups being unmodified, these paramylon derivatives were able to form nanofibers (Kawahara, 2014) by the self-assembly mechanism discussed earlier (Shibakami et al., 2013a). However, a strong decrease of molecular weight was also observed with a final DP = 68 (Tamura et al., 2009). Note that such a small size probably also favours the water solubility. Indeed, underivatized curdlan oligomers with DP = 32, obtained by other authors by hydrolysis with H_2O_2, were also soluble in water (Zhu & Wu, 2019).

Cationic paramylon ether derivatives have been obtained by both homogeneous (Shibakami et al., 2018) and heterogeneous reactions (Daglio et al., 2019). Homogeneous modification was performed in concentrated NaOH aqueous solution with glycidyltrimethylammonium chloride, leading to different DS, from 0.01 to 0.64 depending on the paramylon:ammonium salt ratio (Shibakami et al., 2018). Freeze-dried cationic paramylon samples were put into water showing poor dispersibility for DS < 0.06, and very good solubility for DS > 0.31. For intermediate DS values (0.07 < DS < 0.16) the cationic paramylon chains spontaneously formed nanofibers after dissolution, leading to gelation. Freeze-drying of the gel allowed XRD characterization of the nanofiber whose crystallinity is close to native paramylon, suggesting that the secondary C2

hydroxyl groups, allowing triple helices self-assembly and stabilization, were hardly modified, and that the more reactive C6 OH group was mostly substituted for these intermediate DS (Shibakami et al., 2018). Concurrently, cationic paramylons with DS > 0.31 and DS < 0.06 showed outstanding transparent film forming ability by casting from homogeneous solutions and heterogeneous solutions, respectively (Shibakami et al., 2018). For DS > 0.3 the cationic paramylons may also be used as antidiabetic agents due to their ability to selectively absorb hydrophobic bile salts. Upon administration to diet induced obese mice, a reduction of mesenteric and body fat was observed with a significantly higher secretion of glucagon-like peptide-1 compared to with cellulose reference. (Shibakami, Shibata, et al., 2019).

Recently, higher DS (0.85-1.22) cationic paramylon nanofibers were successfully dispersed in organic solvents such as methanol and binary volatile solvent systems allowing the casting of films (Shibakami, 2021b). Introduction of phenolphthalein showed that, when the films were immersed in alkaline solution, this dye molecule was released faster with increasing DS (Shibakami, 2021b), suggesting potential applications in controlled dye release.

More recently, the heterogeneous modification of paramylon was performed with (3-chloro-2-hydroxypropyl) trimethylammonium chloride (CHPTAC) in water at 90°C, in presence of NaOH and $NaBH_4$ to prevent depolymerisation (Daglio et al., 2019). Only one DS ≈ 0.30 was obtained. In agreement with previous report (Shibakami et al., 2018), this cationic derivative was apparently not fully soluble in water. A solubility in 0.03 $mol.l^{-1}$ Tris/HCl buffer (pH 8.0) is reported (Daglio et al., 2019). However, the modified polysaccharide showed efficient flocculation properties on kaolin suspension, comparable to commercial cationic polyacrylamides (Daglio et al., 2019).

Type	media	reactant type	Reference	Derivative properties
Homogeneous modification				
Anionic.	DMSO(*)	piperidine-N-sulfonic acid (*)	(Koizumi et al., 1993).	Anti HIV activity (1.2 < DS < 1.7)
Anionic	Aqueous NaOH	Chloroacetic acid	(Shibakami et al., 2016; Daglio et al., 2019).	Tablets disintegrant (DS ≈ 0.18-0.25)
cationic	Aqueous NaOH	Glycidilammonium chloride	(Shibakami et al., 2018)	Nanofibers (0.07<DS<0.16) Transparent Solvent cast films (DS > 0.31 or DS < 0.06)
			(Shibakami, 2021b)	Nanofibers dispersible in organic solvents (DS ≈ 1.22) Controlled dye release films
Heterogeneous modifications				
Anionic	2-propanol/Aqueous NaOH mixture	Chloroacetic acid	(Shibakami et al., 2016).	Controlled DS from 0.015 to 0.80 Nanofibers forming ability.
Anionic	Water (pH 10)	TEMPO (regioselective)	(Tamura et al., 2009).	Water-soluble Nanofibers (DS≈1 for C6)
cationic	Water	Chlorinated ammonium chloride	(Daglio et al., 2019)	Flocculant (DS ≈ 0.30)

584 **Table 3**: Paramylon ionic derivatives obtained by homogeneous or heterogeneous reactions in various media (*: not specified by authors,
585 assumed similar to previous anionic modification of curdlan (see text)).

5.2) Paramylon esters derivatives

This section is dedicated to the various modifications involving the substitution of paramylon -OH groups by an ester linkage to a pendant group R= -O- (C=O) – X, which can be of different size and nature (including hydrophobic alkyl chains but also hydrophilic ionic groups).

To our knowledge the first reported modification of this kind was heterogeneous acetylation (X = - CH_3) by reaction with acetic anhydride in a mixture with acetic acid (≈ 2:1 acid/anhydride ratio) with sulfuric acid catalysis (Shibakami et al., 2012). A DS = 0.18 was obtained resulting in the formation of a gel for hydrated paramylon granules, whereas for anhydrous granules, the authors observed the transformation of the shape of the suspended paramylon granules from native spheroidal shape to doughnut-like shape. This unexpected result was ascribed to the solubility of acetylated paramylon in acetic acid, and to the preferential solubilization of the acetylated chains located in the center of the granule, progressively leading to a hole in it (Shibakami et al., 2012). Note that in this case, the "product" is not a paramylon derivative and had no foreseen applications.

In what follows, we will focus first on homogeneous modification reactions, which are the most widely studied, and then on heterogeneous reactions in other media.

5.2.1) Homogenous esterification

The various reported esters and mixed esters of paramylon obtained by homogeneous modification in DMAc/LiCl and DMF/LiCl are listed in **Table 4**. In these solvents of paramylon, the reaction with anhydrides can be conducted in presence of pyridine.

Acetylation leads to different properties depending on the DS. The first report concerns DS > 2.01, leading to semi-crystalline films (Shibakami et al., 2015b): depending on the subsequent purification, acetylated paramylon with different DS were obtained. They were fully soluble in either chloroform (DS =2.01) or dichloromethane (DS = 2.37), allowing the production of self-

standing films by solution casting. The optically transparent films obtained were semi-crystalline, with a higher crystallinity for higher DS, resulting in Young's modulus and elongation at break comparable to those of acetylated cellulose (Shibakami et al., 2015b). However, it should be noted that their crystalline structure was different from that of native paramylon, with the suspected formation of mono helices by these highly acetylated paramylons (Shibakami et al., 2015b). More recently, lower DS values were investigated (Shibakami, 2021a): the same chemical modification conditions were used, but varying reaction time in order to control the DS (Shibakami, 2021a). For the intermediate $1.59 < DS < 2.01$ range, acetylated paramylons displayed a glass transition with a low crystallinity, whereas for lower range ($1.16 < DS < 1.42$) highly crystalline materials, without any observed glass transition, were obtained. Summing up, this suggests the following overall trend for acetylated paramylons: i) high crystallinity similar to pristine paramylon in the lower DS range, ii) lower crystallinity with an amorphous phase for intermediate DS, and iii) increasing crystallinity with presence of mono helices in the higher DS range.

Besides, acetylated paramylon with DS lower than 2 were able to form nanofibers by triple helices self-assembly. For DS = 1.42, nanofibers dispersible and stable in chloroform were obtained, opening perspectives for industrial applications (Shibakami, 2021a). Note that more "classically" water-soluble anionic paramylon esters salts (-X = - CH_2-CH_2-(C=O)-O^- Na^+), able to self-assemble as nanofibers, had previously been obtained by reaction with succinic anhydride in the same homogeneous conditions (in presence of triethylamine), followed by dialyze (Shibakami et al., 2013b). For these succinylated paramylons, the partial DS of the C2, C4 and C6 were 0.23, 0.05 and 0.18, respectively, thus leaving enough intact C2 –OH groups for the formation of triple helices in NaOH solutions (Shibakami et al., 2013b).

Paramylon propionate was also recently obtained by reaction with propionic anhydride (Seok et al., 2021) resulting in DS of 1.6 and 2.0, with a preferential substitution of the C6 primary and C4 secondary hydroxyl groups. These paramylon monoesters were subsequently modified by reacting the C2 hydroxyl group with L-lactide or ε-caprolactone, resulting in poly(lactic acid) (PLA) or polycaprolactone (PCL) grafted side chains. These grafted paramylon derivatives were thermoplastic, with glass transition and melting temperatures close to those of pure PLA and pure PCL, respectively. However, the mechanical properties were significantly lower (Seok et al., 2021). Nevertheless, this approach opens the perspective of making polymer blends between these grafted paramylon esters and pure PLA or PCL.

The above homogeneous acetylation and succinylation reactions with anhydrides were also applied as secondary modifications in order to obtain thermoplastic mixed esters (Shibakami et al., 2014) and amphiphilic mixed esters (Shibakami, 2017). In both cases, paramylon was previously esterified with long hydrophobic pendent chain esters ($-X_1$ = - $(CH_2)_n$-CH_3 ; n=12 or 14 or 16) by reaction with acyl chlorides. This long chain substituent is preferentially substituted to the more reactive C6-OH group, so that the subsequent acetylation or succinylation targets mainly the remaining secondary -OH groups:

- Paramylon acylates succinylated in salt form ($-X_2$ = - CH_2-CH_2-(C=O)-O^- Li^+) were amphiphilic (Shibakami, 2017). Besides still showing ability to self-assemble as nanofibers, these mixed esters induced high viscosity in aqueous solutions, in particular when combining succinylation to higher DS_1 and acyl chain length (Shibakami, 2017). Films prepared by soaking/casting in ethanol combined mechanical strength with optical transparency and remarkable water absorption performances that may be used for medical applications (Shibakami, 2017).
- Concurrently, acetylated paramylon acylates with a total DS in the 2.5 to 2.7 range (acylation DS values were in the 0.28-0.61 range, while acetylation DS was > 2) showed

thermoplastic behavior (Shibakami et al., 2014), with melt flow rates and mechanical properties comparable to commercial bioplastics such PLA and Polyamide11. It is noteworthy that the reversed sequential modification (acetylation followed by acylation) hinders the later due to the higher reactivity of the C6 primary hydroxyl group that, once substituted by acetates, cannot be acylated. This results in a low acylation DS and no thermoplasticity (Shibakami et al., 2014). It suggests that a minimum DS is required in order to obtain thermoplastic paramylon esters. Regarding the type of long chain substituent, the authors insisted on the potential of paramylon acetate myristate for industrial production because of the possibility to obtain myristic acid from *E. gracilis* cultivation in anaerobic conditions (Inui et al., 1983).

Another homogeneous modification strategy for the synthesis of high DS thermoplastic paramylon mixed esters involves the simultaneous "one pot" reaction of paramylon with multiple anhydrides, in the presence of 4-dimethylaminopyridine (Shibakami & Sohma, 2017). It successfully lead to mixed esters with acetate (X_1= -CH_3) and medium chain length acylate (X_2= - $(CH_2)_n$-CH_3) (with n= 1, 2, 3 or 4). Note that the multiple anhydride reactants are obtained by previously mixing one anhydride with one acid: for example, propionic anhydride with acetic acid, or inversely acetic anhydride with propionic acid. However, this affects the final partial DS values, resulting in medium chain length rich or acetyl rich mixed esters with different melt volume rate, melting and glass transition temperatures and mechanical properties. For almost all mixed esters, films could be obtained by hot-pressing at temperatures above 200°C (Shibakami & Sohma, 2017). It was later shown that paramylon acetate propionate can display melt spinnability at 240°C when the partial DS are in the ranges 0.5-0.7 and 2.2-2.5, respectively (Shibakami, Sohma, et al., 2019). The tough monofilaments obtained may be used in medical applications such as sutures.

Reactants	**R= -O- (C=O) – X**	**Reference**	**Derivative properties**
Acetic anhydride	X= $-CH_3$ DS = 2.01-2.37	(Shibakami et al., 2015b)	Transparent self standing films
Acetic anhydride	X=$-CH_3$ DS = 1.16-2.01	(Shibakami, 2021a)	Nanofibers stable in chloroform (DS = 1.42)
Succinic anhydride	X= - CH_2-CH_2-(C=O)-O^- Na^+ DS = 0.46	(Shibakami et al., 2013b)	Water-soluble nanofibers
Propionic anhydride*	X= - (CH_2)-CH_3 DS = 1.60-2.00	(Seok et al., 2021)	Thermoplastic (after grafting with PLA or PCL, see text)
1: Acyl chlorides 2: Acetic anhydride (sequential reactions)	X_1= - $(CH_2)_n$-CH_3 ; n=12,14,16 DS_1 = 0.28-0.61 X_2= $-CH_3$; DS_2 = 2.07-2.49	(Shibakami et al., 2014)	Thermoplastic
1: Acyl chlorides 2: Succinic anhydride (sequential reactions)	X_1= - $(CH_2)_n$-CH_3 ; n=12,14,16 DS_1 up to 0.13 X_2=- CH_2-CH_2-(C=O)-O^- Li^+ or $–CH_3$ DS_2 up to 0.46 (salt) or 2.77 (acetate)	(Shibakami, 2017)	Amphiphilic thickeners Water absorbing films (Acylate Succinate salts)
Multiple anhydrides (simultaneous reactions)	X_1= $-CH_3$ DS_1 = 0.36-1.24 X_2= - $(CH_2)_n$-CH_3 ; n= 1, 2, 3, 4 DS_2 = 1.71-2.24	(Shibakami & Sohma, 2017)	Thermoplastic (hot-press)
Multiple anhydrides (simultaneous reactions)	X_1= $-CH_3$ DS_1 = 0.36-1.24 X_2= - $(CH_2)_n$-CH_3 ; n= 0,1,2 DS_2 = 1.71-2.24	(Shibakami, Sohma, et al., 2019)	Melt spinnable (paramylon acetate proprionate, DS_1 = 0.5-0.7 ; DS_2 = 2.2-2.5)

684 **Table 4**: Paramylon esters and mixed esters obtained by homogeneous esterification reactions in DMAc/LiCl, except * in DMF/LiCl.

5.2.2) Heterogeneous esterification in other media

Heterogeneous esterification of paramylon has also been reported in various media for the production of monoesters and mixed esters (**Table 5**). It allows obtaining high total DS values necessary for thermoplasticity, but with a better control of partial DS values. Thermal transitions, mechanical properties and viscosity can thus be finely tuned. A "one pot" synthesis approach of mixed esters consists in a heterogeneous reaction with two acids in trifluoroacetic anhydride (TFAA) (Shibakami et al., 2015a). Using acetic acid and various long chain fatty acids, the authors observed that the resulting paramylon derivatives (with total DS in the 2.59-2.89 range) are actually soluble in TFAA so that the final solution was homogeneous. The advantage of this approach is that it allows controlling the partial DS by tuning the feed ratio of the two acids. In the case of myristic acid, this allows tuning the thermoplasticity properties of the paramylon acetate myristate (Shibakami et al., 2015a). Indeed a more recent work shows that paramylon acetate myristate with partial DS ≈ 0.35 lead to a good compromise between moldability and mechanical properties, the myristate pendent group acting both as an "internal plasticiser" and a "viscosity increaser" (Shibakami & Sohma, 2020).

This approach was also applied to the synthesis of fully substituted paramylon monoesters with varying pendant chain length (X = - $(CH_2)_n$-CH_3 ; n= 0,1,2,3,4,5,6,7,9,11) (Gan et al., 2017). Total substitution of the paramylon hydroxyl groups was achieved (DS = 3). Depending on the substituted chain length, the thermoplastic polymers were semi-crystalline (n =0-5 with melting temperatures (T_m) values from 281 to 114 °C) or amorphous (n =7-11; the glass transition temperature (T_g) was not measured). Except for the acetate, all these paramylon derivatives were thermoplastic above their glass transition or their melting temperature, allowing hot pressing of films. Film casting from solutions in chloroform was also possible, with similar mechanical properties (Gan et al., 2017). Thermal stretching of the films allowed improving the mechanical performances of the semi-crystalline paramylon monoesters thanks to

orientation. Further investigation of the crystallinity of stretched fibers showed that, contrary to native paramylon, the esterified chains take a 5/1 helical conformation, and that they are arranged in pseudohexagonal unit cells (Gan et al., 2019). This five-fold conformation favors the axial deformation of the fibers, which have low Young's moduli (2.5 to 1 GPa with increasing pendent chain length), especially compared to cellulose triacetates fibers which have a 3/2 helical conformation and Young's moduli ten times higher (Gan et al., 2019).

Partially substituted paramylon monoesters, with DS lower than 3, can be obtained by heterogeneous reaction of acyl chlorides in pyridine (Shibakami & Sohma, 2018). The DS can be controlled in the 1.50 to 3 range by acyl chloride/paramylon ratio. Contrary to fully substituted monoesters, some of these lower DS derivatives were not only thermoplastic, allowing hot pressing of films, but also presented a remarkable tackiness at room temperature. Thus they may be used as pressure sensitive adhesives, with best performances observed for paramylon myristates with DS ≈ 2.6-2.9 (Shibakami & Sohma, 2018).

More recently, the same heterogeneous reaction of acyl chlorides with paramylon was performed in N-methylpyrrolidone/pyridine mixtures (Zhong et al., 2021). DS values from 1.7 to 2.7 were obtained by varying the acyl chloride/paramylon ratio. The authors demonstrated that the DS value can be easily characterized on particles of the paramylon derivatives by terahertz spectroscopy, using specific signature peaks of paramylon which are shifted upon modification (Zhong et al., 2021).

Media	**Reactants**	**R= -O- (C=O) – X**	**Reference**	**Derivative properties**
Acetic acid	Acetic anhydride	X= $-CH_3$; DS=0.18	(Shibakami et al., 2012)	Doughnut-like particles
Trifluoroacetic anhydride	Acetic acid Long chain fatty acids	X_1= $-CH_3$ DS_1 = 1.84-2.24 X_2= - $(CH_2)_n$-CH_3 ; n=6,8,10,12,14,15,16 DS_2=0.35-1.05	(Shibakami et al., 2015a)	Thermoplastic (Acetate Myristate)
Trifluoroacetic anhydride	Various carboxylic acids	X = - $(CH_2)_n$-CH_3 ; n= 0,1,2,3,4,5,6,7,9,11 DS =3	(Gan et al., 2017)	Semi-crystalline thermoplastics (n =1-5) Amorphous thermoplastics (n =7-11) Hot pressed and solvent casted films. Thermally stretched crystalline fibers.
pyridine	Various acyl chlorides	X= - $(CH_2)_n$-CH_3 ; n=12,14,16 DS = 1.5-3	(Shibakami & Sohma, 2018)	Thermoplastic (hot pressed) Pressure sensitive adhesives (paramylon myristates)
N-methylpyrrolidone /pyridine mixture	Various acyl chlorides	X= - $(CH_2)_n$-CH_3 ; n=12,14,16 DS = 1.7-2.7	(Zhong et al., 2021).	Not studied.

730

731 **Table 5**: Paramylon ester derivatives obtained by heterogeneous reactions in various media.

732

Summarizing, compared to pristine paramylon, the various derivatives described throughout this section allow a much wider variety of processing routes: their solvent based processing into films and nanofibers can be done either in water or in organic solvents, thanks to modified solubility, while solvent free thermomechanical processing can become possible thanks to their thermoplasticity without thermal degradation:

- Solubility in water was achieved by substituting paramylon's –OH groups with anionic or cationic groups. The reported minimum DS values are typically lower than 1, but depend strongly on the type of linkage and ionic group. As recalled by one author (Tamura et al., 2009), historically, the first motivation for investigating ionic derivatives was to enhance paramylon's biological activity, whose limited performances were ascribed to its absence of solubility in water. For paramylon sulfates, a correlation is indeed reported between water solubility and bioactivity. However, the optimum DS (1.2-1.7) range is very high compared to that of most of the other anionic and cationic derivatives studied since then. Actually, it is striking that the authors often did not focus on the impact of solubility on their bioactive properties, but rather on their nanofiber forming ability in water (which actually seems to be an efficient way to improve paramylon's bioactive properties, as discussed in section 4 (Sugiyama et al., 2009) (Barsanti & Gualtieri, 2019)) and on the production of films from these nanofibers.

  The reported results suggests that the ability to form nanofibers in water requires the ionic derivatives to combine: i) an absence of, or a low substitution of C2 –OH groups in order to have stable triple helices (this implies a maximum total DS, 1 and 1.22 being the highest reported for regioselective substitution of C6-OH groups, and non regioselective substitution, respectively), and ii) A minimum total DS allowing the destabilization of the native crystalline structure for a partial solubilization before subsequent reassembly as nanofibers. This minimum total DS depends on the ionic

substituent and needs to be finely tuned in order avoid, or favor, gelation of the nanofibers.

- Paramylon acetates can be similarly processed as nanofibers and films in organic solvents. However, this requires higher minimum DS values than for ionic derivatives in water (e.g. in chloroform, solubility is achieved at DS=2.01, while nanofibers are stable of DS=1.42). This may be ascribed to the hydrophilic nature of paramylon's –OH groups, which thus need to be highly substituted. Contrary to pristine paramylon, depending on their DS, paramylon acetates can present a glass transition or a modified crystallinity with presence of mono helices. However, thermoplasticity cannot be achieved, even for DS=3.
- Thermoplasticity requires both a high DS (generally close to 3) and the introduction of at least a fraction of longer aliphatic ester pendant groups allowing to reduce the interactions between paramylon chains by playing an internal plasticiser role. It is striking that the thermoplastic paramylon esters obtained can have melting temperature as high as 280°C, without reported thermal degradation during hot-press processing. This indicates that the substitutions also increase the thermal stability of paramylon. Both mono and mixed esters can be used, with the following apparent rules in terms of DS: i) If only one type of aliphatic ester pendant groups is used, a DS equal to 3 is necessary for short chains (e.g. proprionates), while for long pendant chains (e.g. myristates), the minimum DS can be lowered (down to ≈ 2.5); ii) long pendant chains can also be combined with short chains, including acetates. However, the maximum partial acetylation DS depends on the size of co-substituent: If long pendant chains are used, a rather high partial acetylation can be used (DS ≈ 2), whereas with lower chain length co-subtituents, the maximum acetylation degree that can be tolerated becomes lower, but the total DS should remain close to 3.

Conclusions and perspectives

With the emergence of microalga *E. gracilis* large scale cultivation, the linear β-1,3-glucan paramylon produced by this microorganism is likely to become more and more widely available in the coming years. Due to the high versatility and robustness of euglenoids, paramylon can be produced either in photoautotrophic or heterotrophic (or both), as well as within the framework of environmental-friendly schemes, such as bioremediation, wastewater treatment, and CO_2 trapping. This makes paramylon a potentially carbon neutral and sustainable feedstock for biobased products. However, as a storage polysaccharide, it is biosynthesized as highly crystalline, water insoluble, intracellular granules, in which β-1,3-glucan form stable triple helices. Beside its applications in this raw granular native form, such as dietary fibers, various processing routes have been developed, leading to both non-derivatized and chemically modified paramylon products, with various shapes and properties as summarized in **Figure 3**.

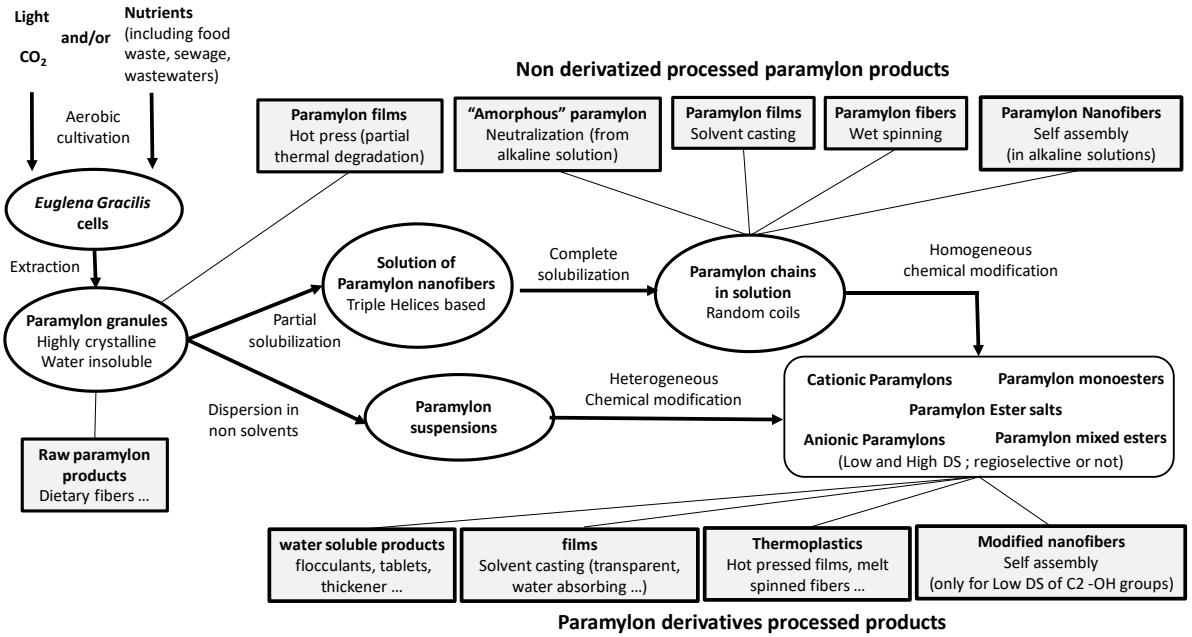

Figure 3: Overview of paramylon processing routes and potential applications.

The use of specific solvents, allowing to disrupt the triple helices, gives the possibility to shape native paramylon into films and fibers without chemical modification. The reversibility of triple

799 helices disruption in aqueous alkaline solutions allows the production of nanofibers by a self-
800 assembly mechanism. This outstanding property of paramylon can persist when paramylon is
801 chemically modified by substitution of hydroxyl groups, except the C2 hydroxyl groups that
802 are involved in triple helices stabilization mechanism. Thus paramylon derivatives based
803 nanofibers can be produced including nanofibers dispersible in organic solvents.

804 Chemical modifications, in homogeneous or heterogeneous conditions, also allows obtaining
805 two classes of paramylon derivatives: i) a variety of water-soluble ionic derivatives particularly
806 interesting for health related applications; and ii) paramylon monoesters and mixed esters,
807 including thermoplastic and melt spinnable derivatives for the production of bioplastic films
808 and fibers.

809 **Suggestions and prospects**

810 Produced as intracellular granules, paramylon first needs to be extracted from *E. gracilis*
811 biomass. However, there is currently no standard method neither for the extraction of the
812 granules, nor for the purification of paramylon. In the perspective of large scale production, it
813 would be necessary to investigate the influence of the extraction and/or of the purification
814 conditions on paramylon's purity and molecular weight. Controlling the purity seems
815 particularly important for the use of paramylon as an immunomodulator, for which the role of
816 other molecules present in *E. gracilis* biomass and paramylon granules needs to be further
817 investigated (Phillips et al., 2019).

818 Regarding the reported solvents of paramylon, it appears that for some of them the exact state
819 of solubilized paramylon, as triple helices or random coils, is not clear. Therefore, it would be
820 interesting to investigate this point, particularly for ionic liquids. Indeed, beside DMSO and
821 concentrated alkaline solutions (which both allow the disruption of triple helices), ionic liquids
822 seem promising new candidates that remain poorly studied, despite their known versatility as

solvents of polysaccharides. Despite their potential influence on paramylon depolymerisation (as observed for curdlan when solubilized in 1-ethyl-3-methylimidazolium acetate) which should be further investigated, ionic liquids present the advantage of being tunable by changing the chemical structure of the anion and cation moieties. These moieties can even be biobased and/or biocompatible. Thus, ionic liquids can potentially be used, not only as solvents for non-derivatising shaping of paramylon or as media for chemical modification, but even as final components of paramylon materials (as plasticisers for example). Last but not least, ionic liquid being efficient solvents of other polysaccharides and biopolymers, they may be used as co-solvent for the processing of blends with paramylon.

Concurrently, the recently reported paramylon monoesters grafted with PCL or PLA chains open perspectives for the melt processing of blends of paramylon derivatives with such polyester bioplastics. The use of derivatised paramylon nanofibers as reinforcements in other polymers would also be interesting to investigate.

Acknowledgements

This project has received financial support from the CNRS through the MITI interdisciplinary program 80Prime.

References

Aida, T. M., Nonaka, T., Fukuda, S., Kujiraoka, H., Kumagai, Y., Maruta, R., Ota, M., Suzuki, I., Watanabe, M. M., Inomata, H., & Smith, R. L. (2016). Nutrient recovery from municipal sludge for microalgae cultivation with two-step hydrothermal liquefaction. *Algal Research*, *18*, 61–68. https://doi.org/10.1016/j.algal.2016.06.009

Aketagawa, J., Tanaka, S., Tamura, H., Shibata, Y., & Saito, H. (1993). Activation of Limulus Coagulation Factor G by Several (l^>3)-#- D-Glucans: Comparison of the Potency of Glucans with Identical Degree of Polymerization but Different Conformations. *J. Biochem.*, *113*(6), 4.

Anraku, M., Iohara, D., Takada, H., Awane, T., Kawashima, J., Takahashi, M., & Hirayama, F. (2020). Morphometric Analysis of Paramylon Particles Produced by *Euglena gracilis* EOD-1 Using FIB/SEM Tomography. *Chemical and Pharmaceutical Bulletin*, *68*(1), 100–102. https://doi.org/10.1248/cpb.c19-00769

Arashida, R., Nakano, R., Suzuki, K., & Yoshida, E. (2011). *Amorphous paramylon* (Patent application No. JP2011184592A).

Arthe, R., Arivuoli, D., & Ravi, V. (2020). Preparation and characterization of bioactive silk fibroin/paramylon blend films for chronic wound healing. *International Journal of Biological Macromolecules*, *154*, 1324–1331. https://doi.org/10.1016/j.ijbiomac.2019.11.010

Bai, W., Shah, F., Wang, Q., & Liu, H. (2019). Dissolution, regeneration and characterization of curdlan in the ionic liquid 1-ethyl-3-methylimidazolium acetate. *International Journal of Biological Macromolecules*, *130*, 922–927. https://doi.org/10.1016/j.ijbiomac.2019.01.223

Barsanti & Gualtieri. (2019). Paramylon, a Potent Immunomodulator from WZSL Mutant of Euglena gracilis. *Molecules*, *24*(17), 3114. https://doi.org/10.3390/molecules24173114

Barsanti, L., Passarelli, V., Evangelista, V., Frassanito, A. M., & Gualtieri, P. (2011). Chemistry, physico-chemistry and applications linked to biological activities of β-glucans. *Natural Product Reports*, *28*(3), 457. https://doi.org/10.1039/c0np00018c

Barsanti, L., Vismara, R., Passarelli, V., & Gualtieri, P. (2001). Paramylon (β-1,3-glucan) content in wild type and WZSL mutant of Euglena gracilis. Effects of growth conditions. *Journal of Applied Phycology*, *13*(1), 59–65. https://doi.org/10.1023/A:1008105416065

Chen, Y., & Wang, F. (2020). Review on the preparation, biological activities and applications of curdlan and its derivatives. *European Polymer Journal*, *141*, 110096. https://doi.org/10.1016/j.eurpolymj.2020.110096

Choi, J. A., Oh, T.-H., Choi, J.-S., Chang, D.-J., & Joo, C.-K. (2013). Impact of β-1,3-glucan Isolated from *Euglena gracilis* on Corneal Epithelial Cell Migration and on Wound Healing in a Rat Alkali Burn Model. *Current Eye Research*, *38*(12), 1207–1213. https://doi.org/10.3109/02713683.2013.811262

874 Chuah, C. T., Sarko, A., Deslandes, Y., & Marchessault, R. H. (1983). Packing analysis of
875 carbohydrates and polysaccharides. Part 14. Triple-helical crystalline structure of curdlan and
876 paramylon hydrates. *Macromolecules*, *16*(8), 1375–1382.
877 https://doi.org/10.1021/ma00242a020
878 Clarke, A. E., & Stone, B. A. (1960). Structure of the paramylon from Euglena gracilis. *Biochimica et*
879 *Biophysica Acta*, *44*, 161–163. https://doi.org/10.1016/0006-3002(60)91534-1
880 Cook, J. R. (1963). Adaptations in Growth and Division in *Euglena* Effected by Energy Supply*. *The*
881 *Journal of Protozoology*, *10*(4), 436–444. https://doi.org/10.1111/j.1550-7408.1963.tb01703.x
882 Daglio, Y., Rodríguez, M. C., Prado, H. J., & Matulewicz, M. C. (2019). Paramylon and synthesis of
883 its ionic derivatives: Applications as pharmaceutical tablet disintegrants and as colloid
884 flocculants. *Carbohydrate Research*, *484*, 107779.
885 https://doi.org/10.1016/j.carres.2019.107779
886 Del Cornò, M., Gessani, S., & Conti, L. (2020). Shaping the Innate Immune Response by Dietary
887 Glucans: Any Role in the Control of Cancer? *Cancers*, *12*(1), 155.
888 https://doi.org/10.3390/cancers12010155
889 Deslandes, Y., Marchessault, R. H., & Sarko, A. (1980). Triple-Helical Structure of(1→3)-β-D-
890 Glucan. *Macromolecules*, 1466–1471.
891 Enomoto-Rogers, Y., Kimura, S., & Iwata, T. (2016). Soft, tough, and flexible curdlan hydrogels and
892 organogels fabricated by covalent cross-linking. *Polymer*, *100*, 143–148.
893 https://doi.org/10.1016/j.polymer.2016.08.032
894 Futatsuyama, H., Yui, T., & Ogawa, K. (1999). Viscometry of Curdlan, a Linear (1→3)-β- D -Glucan,
895 in DMSO or Alkaline Solutions. *Bioscience, Biotechnology, and Biochemistry*, *63*(8), 1481–
896 1483. https://doi.org/10.1271/bbb.63.1481
897 Gan, H., Enomoto, Y., Kabe, T., Ishii, D., Hikima, T., Takata, M., & Iwata, T. (2017). Synthesis,
898 properties and molecular conformation of paramylon ester derivatives. *Polymer Degradation*
899 *and Stability*, *145*, 142–149. https://doi.org/10.1016/j.polymdegradstab.2017.05.011

Gan, H., Kabe, T., Kimura, S., Hikima, T., Takata, M., & Iwata, T. (2019). Crystal structures and crystalline elastic modulus of paramylon esters. *Polymer*, *172*, 7–12. https://doi.org/10.1016/j.polymer.2019.03.002

Gissibl, A., Sun, A., Care, A., Nevalainen, H., & Sunna, A. (2019). Bioproducts From Euglena gracilis: Synthesis and Applications. *Frontiers in Bioengineering and Biotechnology*, *7*, 108. https://doi.org/10.3389/fbioe.2019.00108

GRAS Notice for Paramylon Isolate from Euglena gracilis (ATCC PTA-123017). (2017). FDA. https://www.fda.gov/media/106488/download

Grimm, P., Risse, J. M., Cholewa, D., Müller, J. M., Beshay, U., Friehs, K., & Flaschel, E. (2015). Applicability of Euglena gracilis for biorefineries demonstrated by the production of α-tocopherol and paramylon followed by anaerobic digestion. *Journal of Biotechnology*, *215*, 72–79. https://doi.org/10.1016/j.jbiotec.2015.04.004

Harada, T., Fujimori, K., Hirose, S., & Masada, M. (1966). Growth and *β* -Glucan 10C3K Production by a Mutant of *Alcaligenes faecalis* var. *Myxogenes* in Defined Medium. *Agricultural and Biological Chemistry*, *30*(8), 764–769. https://doi.org/10.1080/00021369.1966.10858682

Inui, H., Miyatake, K., Nakano, Y., & Kitaoka, S. (1983). Production and Composition of Wax Esters by Fermentation of *Euglena gracilis*. *Agricultural and Biological Chemistry*, *47*(11), 2669–2671. https://doi.org/10.1080/00021369.1983.10866013

Jeon, M. S., Han, S.-I., Kim, J. Y., & Choi, Y.-E. (2020). Co-cultivation of Euglena gracilis and Pseudoalteromonas sp. MEBiC 03607 for paramylon production. *Journal of Applied Phycology*. https://doi.org/10.1007/s10811-020-02215-z

Kataoka, K., Muta, T., Yamazaki, S., & Takeshige, K. (2002). Activation of Macrophages by Linear (1→3)-β-d-Glucans: IMPLICATIONS FOR THE RECOGNITION OF FUNGI BY INNATE IMMUNITY. *Journal of Biological Chemistry*, *277*(39), 36825–36831. https://doi.org/10.1074/jbc.M206756200

Kawahara, Y. (2014). (1→3)-β-d-Glucan nanofibers from paramylon via electrospinning. *Carbohydrate Polymers*, *112*, 73–76. https://doi.org/10.1016/j.carbpol.2014.05.066

927 Kawahara, Y., & Koganemaru, A. (2006). Development of novel film using paramylon prepared
928 fromEuglena gracilis. *Journal of Applied Polymer Science*, *102*(4), 3495–3497.
929 https://doi.org/10.1002/app.24618
930 Kawahara, Y., Ohtani, T., & Nakamura, M. (2020). Direct Resinification of Two (1→3)-β-D-Glucans,
931 Curdlan and Paramylon, via Hot-Press Compression Molding. *Publication Cover Journal of*
932 *Macromolecular Science, Part B*, 635–647.
933 Kim, J. Y., Oh, J.-J., Kim, D. H., Park, J., Kim, H. S., & Choi, Y.-E. (2020). Rapid and Accurate
934 Quantification of Paramylon Produced from Euglena gracilis Using an ssDNA Aptamer.
935 *Journal of Agricultural and Food Chemistry*, *68*(1), 402–408.
936 https://doi.org/10.1021/acs.jafc.9b04588
937 Kiss, J. Z., Roberts, E. M., Brown, R. M., & Triemer, R. E. (1988). X-ray and dissolution studies of
938 paramylon storage granules fromEuglena. *Protoplasma*, *146*(2), 150–156.
939 https://doi.org/10.1007/BF01405924
940 Kiss, J. Z., Vasconcelos, A. C., & Triemer, R. E. (1987). STRUCTURE OF THE EUGLENOID
941 STORAGE CARBOHYDRATE, PARAMYLON. *American Journal of Botany*, *74*(6), 877–
942 882. https://doi.org/10.1002/j.1537-2197.1987.tb08691.x
943 Kobayashi, K., Kimura, S., Togawa, E., Wada, M., & Kuga, S. (2010). Crystal transition of paramylon
944 with dehydration and hydration. *Carbohydrate Polymers*, *80*(2), 491–497.
945 https://doi.org/10.1016/j.carbpol.2009.12.009
946 Koizumi, N., Sakagami, H., Utsumi, A., Fujinaga, S., Takeda, M., Asano, K., Sugawara, I., Ichikawa,
947 S., Kondo, H., Mori, S., Miyatake, K., Nakano, Y., Nakashima, H., Murakami, T., Miyano,
948 N., & Yamamoto, N. (1993). Anti-HIV (human immunodeficiency virus) activity of sulfated
949 paramylon. *Antiviral Research*, *21*(1), 1–14. https://doi.org/10.1016/0166-3542(93)90063-O
950 Kottuparambil, S., Thankamony, R. L., & Agusti, S. (2019). Euglena as a potential natural source of
951 value-added metabolites. A review. *Algal Research*, *37*, 154–159.
952 https://doi.org/10.1016/j.algal.2018.11.024

Krajčovič, J., Matej Vesteg, & Schwartzbach, S. D. (2015). Euglenoid flagellates: A multifaceted biotechnology platform. *Journal of Biotechnology*, *202*, 135–145. https://doi.org/10.1016/j.jbiotec.2014.11.035

Kusmic, C., Barsanti, L., Di Lascio, N., Faita, F., Evangelista, V., & Gualtieri, P. (2018). Anti-fibrotic effect of paramylon nanofibers from the WZSL mutant of Euglena gracilis on liver damage induced by CCl 4 in mice. *Journal of Functional Foods*, *46*, 538–545. https://doi.org/10.1016/j.jff.2018.05.021

Manners, D., Ryley, J., & Stark, J. (1966). Studies on the metabolism of the protozoa. The molecular structure of the reserve polysaccharide from Astasia ocellata. *Biochemical Journal*, *101*(2), 323–327. https://doi.org/10.1042/bj1010323

Marchessault, R. H., & Deslandes, Y. (1979). Fine structure of (1→3)-β-d-glucans: Curdlan and paramylon. *Carbohydrate Research*, 231–242.

Marchessault, R. H., Deslandes, Y., Ogawa, K., & Sundararajan, P. R. (1977). X-Ray diffraction data for β-(1 → 3)- D -glucan. *Canadian Journal of Chemistry*, *55*(2), 300–303. https://doi.org/10.1139/v77-045

Matsuda, F., Hayashi, M., & Kondo, A. (2011). Comparative Profiling Analysis of Central Metabolites in *Euglena gracilis* under Various Cultivation Conditions. *Bioscience, Biotechnology, and Biochemistry*, *75*(11), 2253–2256. https://doi.org/10.1271/bbb.110482

Matsumoto, Y., Enomoto, Y., Kimura, S., & Iwata, T. (2021). Highly deformable and recoverable cross-linked hydrogels of 1,3-α-d and 1,3-β-d-glucans. *Carbohydrate Polymers*, *251*, 116794. https://doi.org/10.1016/j.carbpol.2020.116794

McIntosh, M., Stone, B. A., & Stanisich, V. A. (2005). Curdlan and other bacterial (1→3)-β-d-glucans. *Applied Microbiology and Biotechnology*, *68*(2), 163–173. https://doi.org/10.1007/s00253-005-1959-5

Meeuse, B. (1964). Breakdown of paramylon and laminarin by digestive enzymes of Lamellibranchs—An important ecological feature. *Basteria*, 67–69.

Miyoshi, K., Uezu, K., Sakurai, K., & Shinkai, S. (2004). Proposal of a New Hydrogen-Bonding Form to Maintain Curdlan Triple Helix. *Chemistry & Biodiversity*, *1*(6), 916–924. https://doi.org/10.1002/cbdv.200490073

Monfils, A. K., Triemer, R. E., & Bellairs, E. F. (2011). Characterization of paramylon morphological diversity in photosynthetic euglenoids (Euglenales, Euglenophyta). *Phycologia*, *50*(2), 156–169. https://doi.org/10.2216/09-112.1

Muñóz-Almagro, N., Gilbert-López, B., M. Carmen, P.-R., García-Fernandez, Y., Almeida, C., Villamiel, M., Mendiola, J. A., & Ibáñez, E. (2020). Exploring the Microalga Euglena cantabrica by Pressurized Liquid Extraction to Obtain Bioactive Compounds. *Marine Drugs*, *18*(6), 308. https://doi.org/10.3390/md18060308

Okuyama, K., Otsubo, A., Fukuzawa, Y., Ozawa, M., Harada, T., & Kasai, N. (1991). Single-Helical Structure of Native Curdlan and its Aggregation State. *Journal of Carbohydrate Chemistry*, 645–656.

Phillips, F. C., Jensen, G. S., Showman, L., Tonda, R., Horst, G., & Levine, R. (2019). Particulate and solubilized β-glucan and non-β-glucan fractions of Euglena gracilis induce pro- and anti-inflammatory innate immune cell responses and exhibit antioxidant properties. *Journal of Inflammation Research*, *Volume 12*, 49–64. https://doi.org/10.2147/JIR.S191824

Piiparinen, J., Barth, D., Eriksen, N. T., Teir, S., Spilling, K., & Wiebe, M. G. (2018). Microalgal CO2 capture at extreme pH values. *Algal Research*, *32*, 321–328. https://doi.org/10.1016/j.algal.2018.04.021

Quesada, L., de Lustig, E., Marechal, L., & Belcopito, E. (1976). Antitumor activity of paramylon on sarcoma-180 in mice. *Gann, The Japanese Journal of Cancer Research*, 455–459.

Rodríguez-Zavala, J. S., Ortiz-Cruz, M. A., Mendoza-Hernández, G., & Moreno-Sánchez, R. (2010). Increased synthesis of α-tocopherol, paramylon and tyrosine by Euglena gracilis under conditions of high biomass production: Metabolites biosynthesis by E. gracilis. *Journal of Applied Microbiology*, *109*(6), 2160–2172. https://doi.org/10.1111/j.1365-2672.2010.04848.x

Rubiyatno, Matsui, T., Mori, K., & Toyama, T. (2021). Paramylon production by Euglena gracilis via mixotrophic cultivation using sewage effluent and waste organic compounds. *Bioresource Technology Reports*, *15*, 100735. https://doi.org/10.1016/j.biteb.2021.100735

Russo, R., Barsanti, L., Evangelista, V., Frassanito, A. M., Longo, V., Pucci, L., Penno, G., & Gualtieri, P. (2017). Euglena gracilis paramylon activates human lymphocytes by upregulating pro-inflammatory factors. *Food Science & Nutrition*, *5*(2), 205–214. https://doi.org/10.1002/fsn3.383

Šantek, B., Friehs, K., Lotz, M., & Flaschel, E. (2012). Production of paramylon, a β-1,3-glucan, by heterotrophic growth of Euglena gracilis on potato liquor in fed-batch and repeated-batch mode of cultivation. *Engineering in Life Sciences*, *12*(1), 89–94. https://doi.org/10.1002/elsc.201100025

Scartazza, A., Picciarelli, P., Mariotti, L., Curadi, M., Barsanti, L., & Gualtieri, P. (2017). The role of *Euglena gracilis* paramylon in modulating xylem hormone levels, photosynthesis and water-use efficiency in *Solanum lycopersicum* L. *Physiologia Plantarum*, *161*(4), 486–501. https://doi.org/10.1111/ppl.12611

Seok, J. H., Enomoto, Y., & Iwata, T. (2021). Synthesis and characterization of paramylon propionate-graft- poly(lactic acid) and paramylon propionate-graft-poly(ε-caprolactone). *Polymer*, *228*, 123922. https://doi.org/10.1016/j.polymer.2021.123922

Shibakami, M. (2017). Thickening and water-absorbing agent made from euglenoid polysaccharide. *Carbohydrate Polymers*, *173*, 451–464. https://doi.org/10.1016/j.carbpol.2017.06.025

Shibakami, M. (2021a). Nanofibers made from acetylparamylons by a soaking method. *Polymer*, *220*, 123563. https://doi.org/10.1016/j.polymer.2021.123563

Shibakami, M. (2021b). Organic-solvent-dispersible paramylon nanofibers: Hygroscopicity and extended dye release from its cast films. *Polymer*, *230*, 124082. https://doi.org/10.1016/j.polymer.2021.124082

Shibakami, M., Nemoto, T., & Sohma, M. (2018). Dependence of dissolution, dispersion, and aggregation characteristics of cationic polysaccharides made from euglenoid β-1,3-glucan on

degree of substitution. *Cellulose*, *25*(4), 2217–2234. https://doi.org/10.1007/s10570-018-1740-4

Shibakami, M., Shibata, K., Akashi, A., Onaka, N., Takezaki, J., Tsubouchi, G., & Yoshikawa, H. (2019). Creation of Straight-Chain Cationic Polysaccharide-Based Bile Salt Sequestrants Made from Euglenoid β-1,3-Glucan as Potential Antidiabetic Agents. *Pharmaceutical Research*, *36*(1), 23. https://doi.org/10.1007/s11095-018-2553-8

Shibakami, M., & Sohma, M. (2017). Synthesis and thermal properties of paramylon mixed esters and optical, mechanical, and crystal properties of their hot-pressed films. *Carbohydrate Polymers*, *155*, 416–424. https://doi.org/10.1016/j.carbpol.2016.08.093

Shibakami, M., & Sohma, M. (2018). Thermal, crystalline, and pressure-sensitive adhesive properties of paramylon monoesters derived from an euglenoid polysaccharide. *Carbohydrate Polymers*, *200*, 239–247. https://doi.org/10.1016/j.carbpol.2018.08.005

Shibakami, M., & Sohma, M. (2020). Effects of Long-Chain Acyl Substituents on the Thermoplasticity and Mechanical Properties of Paramylon Mixed Esters. *Journal of Polymers and the Environment*, *28*(8), 2263–2276. https://doi.org/10.1007/s10924-020-01763-2

Shibakami, M., Sohma, M., & Hayashi, M. (2012). Fabrication of doughnut-shaped particles from spheroidal paramylon granules of Euglena gracilis using acetylation reaction. *Carbohydrate Polymers*, *87*(1), 452–456. https://doi.org/10.1016/j.carbpol.2011.08.012

Shibakami, M., Sohma, M., Kijima, N., & Nemoto, T. (2019). Melt spinnabilities of thermoplastic paramylon mixed esters. *Heliyon*, *5*(11), e02843. https://doi.org/10.1016/j.heliyon.2019.e02843

Shibakami, M., Tsubouchi, G., & Hayashi, M. (2014). Thermoplasticization of euglenoid β-1,3-glucans by mixed esterification. *Carbohydrate Polymers*, *105*, 90–96. https://doi.org/10.1016/j.carbpol.2014.01.053

Shibakami, M., Tsubouchi, G., Nakamura, M., & Hayashi, M. (2013a). Polysaccharide nanofiber made from euglenoid alga. *Carbohydrate Polymers*, *93*(2), 499–505. https://doi.org/10.1016/j.carbpol.2012.12.040

1059 Shibakami, M., Tsubouchi, G., Nakamura, M., & Hayashi, M. (2013b). Preparation of carboxylic acid-
1060 bearing polysaccharide nanofiber made from euglenoid β-1,3-glucans. *Carbohydrate*
1061 *Polymers*, *98*(1), 95–101. https://doi.org/10.1016/j.carbpol.2013.05.026
1062 Shibakami, M., Tsubouchi, G., Sohma, M., & Hayashi, M. (2015a). One-pot synthesis of
1063 thermoplastic mixed paramylon esters using trifluoroacetic anhydride. *Carbohydrate*
1064 *Polymers*, *119*, 1–7. https://doi.org/10.1016/j.carbpol.2014.11.036
1065 Shibakami, M., Tsubouchi, G., Sohma, M., & Hayashi, M. (2015b). Preparation of transparent self-
1066 standing thin films made from acetylated euglenoid β-1,3-glucans. *Carbohydrate Polymers*,
1067 *133*, 421–428. https://doi.org/10.1016/j.carbpol.2015.06.104
1068 Shibakami, M., Tsubouchi, G., Sohma, M., & Hayashi, M. (2016). Synthesis of nanofiber-formable
1069 carboxymethylated Euglena -derived β-1,3-glucan. *Carbohydrate Polymers*, *152*, 468–478.
1070 https://doi.org/10.1016/j.carbpol.2016.06.100
1071 Simon, R. R., Vo, T. D., & Levine, R. (2016). Genotoxicity and subchronic toxicity evaluation of
1072 dried Euglena gracilis ATCC PTA-123017. *Regulatory Toxicology and Pharmacology*, *80*,
1073 71–81. https://doi.org/10.1016/j.yrtph.2016.06.007
1074 Skov, J., Kania, P. W., Holten-Andersen, L., Fouz, B., & Buchmann, K. (2012). Immunomodulatory
1075 effects of dietary β-1,3-glucan from Euglena gracilis in rainbow trout (Oncorhynchus mykiss)
1076 immersion vaccinated against Yersinia ruckeri. *Fish & Shellfish Immunology*, *33*(1), 111–120.
1077 https://doi.org/10.1016/j.fsi.2012.04.009
1078 Sletmoen, M., & Stokke, B. T. (2008). Higher order structure of (1,3)-β-D-glucans and its influence on
1079 their biological activities and complexation abilities. *Biopolymers*, *89*(4), 310–321.
1080 https://doi.org/10.1002/bip.20920
1081 Stone, B. A. (2009). Chemistry of β-Glucans. In *Chemistry, Biochemistry, and Biology of 1-3 Beta*
1082 *Glucans and Related Polysaccharides* (pp. 5–46). Elsevier. https://doi.org/10.1016/B978-0-
1083 12-373971-1.00002-9
1084 Sugiyama, A., Hata, S., Suzuki, K., Yoshida, E., Nakano, R., Mitra, S., Arashida, R., Asayama, Y.,
1085 Yabuta, Y., & Takeuchi, T. (2010). Oral Administration of Paramylon, a .BETA.-1,3-D-
1086 Glucan Isolated from Euglena gracilis Z Inhibits Development of Atopic Dermatitis-Like Skin

Lesions in NC/Nga Mice. *Journal of Veterinary Medical Science*, *72*(6), 755–763. https://doi.org/10.1292/jvms.09-0526

Sugiyama, A., Suzuki, K., Mitra, S., Arashida, R., Yoshida, E., Nakano, R., Yabuta, Y., & Takeuchi, T. (2009). Hepatoprotective Effects of Paramylon, a .BETA.-1,3-D-Glucan Isolated from Euglena gracilis Z, on Acute Liver Injury Induced by Carbon Tetrachloride in Rats. *Journal of Veterinary Medical Science*, *71*(7), 885–890. https://doi.org/10.1292/jvms.71.885

Suzuki, S., Togo, A., Gan, H., Kimura, S., & Iwata, T. (2021). Air-Jet Wet-Spinning of Curdlan Using Ionic Liquid. *ACS Sustainable Chemistry & Engineering*, *9*(11), 4247–4255. https://doi.org/10.1021/acssuschemeng.1c00488

Tamura, N., Wada, M., & Isogai, A. (2009). TEMPO-mediated oxidation of (1→3)-β-d-glucans. *Carbohydrate Polymers*, *77*(2), 300–305. https://doi.org/10.1016/j.carbpol.2008.12.040

Tanaka, Y., Ogawa, T., Maruta, T., Yoshida, Y., Arakawa, K., & Ishikawa, T. (2017). Glucan synthase-like 2 is indispensable for paramylon synthesis in *Euglena gracilis*. *FEBS Letters*, *591*(10), 1360–1370. https://doi.org/10.1002/1873-3468.12659

Vogel, K., & Barber, A. A. (1968). Degradation of Paramylon by Euglena gracilis. *The Journal of Protozoology*, *15*(4), 657–662. https://doi.org/10.1111/j.1550-7408.1968.tb02189.x

Wakisaka, Y., Suzuki, Y., Iwata, O., Nakashima, A., Ito, T., Hirose, M., Domon, R., Sugawara, M., Tsumura, N., Watarai, H., Shimobaba, T., Suzuki, K., Goda, K., & Ozeki, Y. (2016). Probing the metabolic heterogeneity of live Euglena gracilis with stimulated Raman scattering microscopy. *Nature Microbiology*, *1*(10). https://doi.org/10.1038/nmicrobiol.2016.124

Watanabe, T., Shimada, R., Matsuyama, A., Yuasa, M., Sawamura, H., Yoshida, E., & Suzuki, K. (2013). Antitumor activity of the β-glucan paramylon from Euglena against preneoplastic colonic aberrant crypt foci in mice. *Food & Function*, *4*(11), 1685. https://doi.org/10.1039/c3fo60256g

Yan, J.-K., Cai, W.-D., Wang, C., Yu, Y.-B., Zhang, H.-N., Yang, Y., & Wang, W.-H. (2020). Macromolecular behavior, structural characteristics and rheological properties of alkali-neutralization curdlan at different concentrations. *Food Hydrocolloids*, *105*, 105785. https://doi.org/10.1016/j.foodhyd.2020.105785

Yasuda, K., Ogushi, M., Nakashima, A., Nakano, Y., & Suzuki, K. (2018). Accelerated Wound Healing on the Skin Using a Film Dressing with β-Glucan Paramylon. *In Vivo*, *32*(4), 799–805. https://doi.org/10.21873/invivo.11310

Yoshida, T., Hatanaka, K., Uryu, T., Kaneko, Y., Suzuki, E., Miyano, H., Mimura, T., Yoshida, O., & Yamamoto, N. (1990). Synthesis and structural analysis of curdlan sulfate with a potent inhibitory effect in vitro of AIDS virus infection. *Macromolecules*, 3717–3722.

Zhong, J., Mori, T., Kashiwagi, T., Yamashiro, M., Kusunose, S., Mimami, H., Tsujimoto, M., Tanaka, T., Kawashima, H., Nakagawa, S., Ito, J., Kijima, M., Iji, M., Watanabe, M. M., & Kadowaki, K. (2021). Characteristic terahertz absorption spectra of paramylon and paramylon-ester compounds. *Spectrochimica Acta Part A: Molecular and Biomolecular Spectroscopy*, *244*, 118828. https://doi.org/10.1016/j.saa.2020.118828

Zhu, Q., & Wu, S. (2019). Water-soluble β-1,3-glucan prepared by degradation of curdlan with hydrogen peroxide. *Food Chemistry*, *283*, 302–304. https://doi.org/10.1016/j.foodchem.2019.01.036